A MICROSCOPIC DESCRIPTION of HYPERNUCLEUS PRODUCTION using FAST KAONS

by

Robert J. Esch

B. Sc. (Hon.), University of Guelph, 1970

A THESIS SUBMITTED IN PARTIAL FULFILMENT OF

THE REQUIREMENTS FOR THE DEGREE OF

MASTER OF SCIENCE

in the department

of

PHYSICS

We accept this thesis as conforming to the required standard

THE UNIVERSITY OF BRITISH COLUMBIA

APRIL, 1972

In presenting this thesis in partial fulfilment of the requirements for an advanced degree at the University of British Columbia, I agree that the Library shall make it freely available for reference and study. I further agree that permission for extensive copying of this thesis for scholarly purposes may be granted by the Head of my Department or by his representatives. It is understood that copying or publication of this thesis for financial gain shall not be allowed without my written permission.

Department of PHYSICS

The University of British Columbia
Vancouver 8, Canada

Date 6 April, 1972

To my wife, Rosemary

Preface and Acknowledgements

In the first year of my studies, Professor Vogt and I worked on such varied problems as low energy nuclear reactions, nuclear astrophysics and medium energy pion physics. Needless to say I received exposure to many varied problems in physics. Because Professor Vogt was to go on Sabbatical the following year, he personally made arrangements with the National Research Council of Canada, The Department of Physics, U.B.C. and the Department of Theoretical Physics, Oxford, so that I could go to England with him. Shortly after arriving in Oxford, Dr. N. Tanner of the Department of Nuclear Physics, Oxford, informed us of the need for the calculations out of which this work arose.

I would personally like to thank several friends for their help and encouragement:

To my friend and teacher, Professor Erich Vogt, for his help, patience, and encouragement throughout the course of this work;

Dr. N. Tanner, who pointed out the need for these calculations and for his constant help and encouragement and to

Dr. R. Rook, who calculated the lambda wave function and for his interest in the problem.

I would also like to thank Professor R. E. Peierls and Professor E. Vogt for making it possible to come to Oxford; the National Research Council of Canada for support through a 1967 Science Scholarship and the Oxford Computing Center where most of the calculations were performed.

Finally, and above all, I wish to express my gratitude to my wife, Rosemary, for carefully typing the thesis and without whose constant patience, love and encouragement this work would not have been possible.

<u>TABLE OF CONTENTS</u>

ABSTRACT

The differential cross sections for the production of definite lambda hypernuclear states, within the single scattering, impulse approximation, are calculated from the reaction $n(K^-,\pi^-)\Lambda^0$ on nuclear targets of helium, carbon and oxygen at various K-meson incident momentum. It is shown that these predictions are very sensitive to the three momentum transfer and to the wave function of the bound lambda in the hypernucleus. From the calculations, it is shown that it is possible to observe their production by studying the missing mass spectrum of the emitted pion.

Introduction Chapter 1

The production and study of hypernuclei has been and continues to be a very fruitful and exciting overlap between nuclear and particle physics. Since the early fifties, hypernuclear physics has provided basic information concerning the lambda-hyperon-nucleon interactions and hypernuclear studies have also supplied the nuclear physicist with information basic to understanding nucleon-nucleon forces in matter (Davis, D.H. and Sacton, J., 1967 and references therein).

Unfortunately, however, their production has largely been limited to manufacture from slow negative K-mesons, which are captured in Coulomb orbits about a nucleus. The captured K-meson cascades down toward its atomic (1s) orbital. As it does, it has a larger and larger overlap with the nucleus. But because the K-meson reacts strongly with nucleons, the cascading kaon is absorbed by the nucleus. The energy released in the reaction $n(K^-,\pi^-)\Lambda^\circ$ may leave the produced lambda-hyperon in the nucleus, in some "bound" state or more often both the lambda and pion will escape, leaving an excited nucleus. The nucleus may even "explode", perhaps producing a hypernucleus fragment. The life and death of hypernuclei are usually recorded by the tracks left (before and after decay) in emulsion photographs. It is the study and analysis of these tracks that have yielded binding energies, angular distributions, and branching ratios of decay channels. This data has then been used to study, phenomenologically, the lambda-nucleon force and nucleon-nucleon forces in nuclei. From this theory, it is possible to make models of the hypernucleus states and to check nuclear models.

Capture from Coulomb bound orbits is the easiest way to make hypernuclei, but the process has an unfortunate drawback. In the capture of a K-meson at rest, the momentum transfer to the lambda is typically 250 MeV/c. As a result, the production rate from captured K-mesons is limited to less than 2% for all stopped kaons. For example, in ^{12}C, only one in approximately 350 K-mesons that are captured in Coulomb orbits produce lambda hypernuclei (Davis, D.H. and Sacton, J., 1967). This is quite easy to understand when one considers what the production rate will depend upon. If one can consider the reaction $^{12}C(K^-,\pi^-)^{12}C_\Lambda$ occurring with only a single nucleon, the production rate will be roughly proportional to the Fourier transofrm of the product of the struck neutron and the final bound lambda wave functions. But because the lambda is bound (for p-shell hypernuclei) by only $\sim$ 10MeV, in its s-state, the high momentum components in the form factor will be suppressed. As a result, the production rate will be reduced. This method makes it almost impossible to study excited hypernuclear states if they exist.

In order to study hypernuclei and their excited states, this problem of high momentum transfer must be overcome. Dalitz (Dalitz, R.H., 1969) proposed that it may be possible to study hypernuclear levels, by using "fast"kaon beams of approximately 600 MeV/c. The reaction

$$K^- + n \longrightarrow \Lambda^\circ + \pi^- \quad (1)$$

at 600 MeV/c has one very encouraging feature. When the incident kaon has roughly 550 MeV/c, the emitted pion comes off with 550 MeV/c momentum at zero degrees and hence the produced Λ° comes at rest in the laboratory. Thus, at these incident momenta, it is possible to "deposit" a lambda into the nuclear system. This peculiar behaviour in the kinematics is basically because the reaction (1) is strongly exothermic with a Q value of

178.19 MeV. This method for producing hypernuclei has become known as "producing hypernuclei with <u>walking</u> lambdas", (Bonazzola, G.C. et al, 1970). By detecting the pions emitted at forward angles in the reaction

$$K^- + \text{nucleus} \longrightarrow \text{hypernucleus} + \pi^-$$

the determination of hypernuclear levels can then be made from a direct kinematical analysis for the missing mass or energy loss. The missing mass then gives, the binding energies of the hypernuclear levels produced. For excited states, if production rates are appreciable, more complex decay schemes of the hypernucleus will be available for study, by using γ -rays in coincidence with the emitted pions (Bonazzola, G.C. et al, 1970).

One can estimate that the total differential cross section for reaction will be given by

$$\left(\frac{d\sigma}{d\Omega}\right)_{hyper.} \doteq N_{eff}(A, \sigma_1, \sigma_2)\left(\frac{d\sigma}{d\Omega}\right)_{free} \tag{2}$$

where $(d\sigma/d\Omega)$free is the differential cross section for reaction (1) at the same incident K-meson momentum and $N_{eff}(A, \sigma_1, \sigma_2)$ the effective neutron number (Kolbig, K.S., Margolis, B., 1968). This estimate contains a sum over all possible final states and also contains approximate absorptive and multiple scattering effects in $N_{eff}(A, \sigma_1, \sigma_2)$, σ_1 is the total K-N cross section, σ_2 the π-N total cross section. Calculations for a uniform sphere model for O^{16} reduce the effective number of p-shell neutrons from 6 to 1.85 ($\sim$ 2). $(d\sigma/d\Omega)$free at 600 MeV/c 0°, is 4mb/st (lab). From this model one gets that the $(d\sigma/d\Omega)$hyper. at 0° is roughly 8 mb/st. Neglecting multiple scattering and absorptive effects $(d\sigma/d\Omega)$ hyper. at 0° is $\sim$24 mb/st. The true answer will probably fall between these two estimates.

With only these rough estimates available and the experiments scheduled to start in the spring of this year, it became interesting to make more accurate estimates for the differential cross sections and to study not the closure approximation to $(d\sigma/d\Omega)$hyper., but the contribution from various hypernuclear states (Tanner, N. 1971). It is to these questions that the present work is addressed.

The differential cross sections for hypernucleus production on ^{4}He, ^{12}C and ^{16}O have been calculated in the single scattering, impulse approximation at incident momenta 500, 600, 700 and 800 MeV/c to definite hypernucleus states.

The predictions made here are found to be very sensitive to the momentum transfered to the bound lambda and to the wave function of the lambda.

The treatment presented here consists of essentially four steps:

(1) phenomological description of reaction (1) at incident K-meson lab. momenta 500, 600, 700 and 800 MeV/c;

(2) a proper treatment of the nuclear wave function, including antisymmetry;

(3) some appropriate description of the Λ-hyperon wave function and

(4) a proper treatment of kinematics in the initial and final states.

When these steps are completed, they can be put together under the single scattering impulse approximation (Appendix 1) to yield theoretical estimates for the production of various hypernuclear energy levels at forward angles.

Chapter 2 Reaction $n(K^-,\pi^-)\Lambda^0$

In the description of hypernucleus production, as in all descriptions for the interaction of a particle with a many particle system, it is necessary to relate in some logical way, the elementary two body interactions to the total target-projectile interaction. In the formal theory of multiple scattering (Goldberger, M.L. and Watson, K.M., 1964), the single scattering impulse approximation tells one that the inelastic or collision cross section will be essentially the product of three factors: (1) the number of effective scatterers, (2) the inelastic form factor squared and (3) the elementary free two body differential cross section. The structure of the target has no dynamical effect on the process except in a trivial kinematical way (see Appendix 1) and (Figure 1). In this section, we present the information concerning the free differential cross section for the reaction which is necessary for our theoretical prediction of the hypernucleus production cross section.

At low energies (less than 300 MeV/c. kaon momentum) the reaction $n(K^-,\pi^-)\Lambda$ is predominantly s-wave and has been extensively discussed (Källén, G., 1964). In the region between 300 MeV/c. to 600 MeV/c. the experiments have been scarce and not a great deal is known, but p-wave effects are noticeable. From 600 MeV/c. to 800 MeV/c., the experimental data is not very good but fits to the differential cross sections have been made by expanding the differential cross section in terms of Legendre polynomials of the cosine of the scattering angle in the center of mass

$$\left(\frac{d\sigma}{d\Omega}\right) = \frac{2}{(k)^2}\sum_{n=0}^{\infty} A_n P_n(\cos\theta) \tag{3}$$

with k the momentum in the center of mass $(\hbar = c = 1)$. The coefficients are incident momentum dependent and the Legendre polynomial coefficients versus incident K-meson momentum are shown in Fig. 2 (Armenteros, R. et al, 1968). In Fig. 3 the experimental differential cross section is shown for reaction (1) at 777 MeV/c. incident kaon momentum. From these graphs it is clear that the reaction in the momentum range 500 - 800 MeV/c. is predominately s-wave and p-wave with little interference between them. Briefly, if we expand the scattering amplitude $f(k,\theta)$ in terms of Legendre polynomials and keep only terms up to $\ell = 1$, one has

(4) $$f(k,\theta) = \frac{1}{2ik}\left\{(\eta_0 e^{2i\delta_0} - 1) + 3(\eta_1 e^{2i\delta_1} - 1)\cos\theta\right\} .$$

The differential cross section is $|f(k,\theta)|^2$. To this order

(5) $$\left(\frac{d\sigma}{d\Omega}\right)_{free} = \frac{2}{(k)^2}\left\{A_0 + A_1\cos\theta + A_2\left(\frac{3}{2}\cos^2\theta - \frac{1}{2}\right)\right\} .$$

From the Fig. 2, A_1 for reaction (1) is approximately zero and in this work, it was taken as identically zero. This is not necessary but it simplifies the work without introducing a significant error.

Now from relativistic scattering theory, the differential cross section in the center of mass is given by

(6) $$\left(\frac{d\sigma}{d\Omega}\right) = \frac{1}{64\pi^2 s}\left|\frac{k_f}{k}\right| |t|^2$$
$$= \frac{1}{64\pi^2 s}\sqrt{\frac{\lambda(s, m_\pi^2, m_\Lambda^2)}{\lambda(s, m_K^2, m_n^2)}}\ |t|^2$$

where s is the square of the total energy in the center of momentum, k_f, k are final and initial momentum and

(7) $$\lambda(x,y,z) = x^2 + y^2 + z^2 - 2xy - 2yz - 2xz .$$

From equations (5) and (6), the square of the absolute value of the free two body transition amplitude is

(8) $$|t|^2 = \frac{64\pi^2 s}{k\,k_f}\sum_n A_n(k)\,P_n(\cos\theta)$$

In the calculations, that have been completed, we used the experimental fit to the free two body transition amplitude. The coefficients are momentum dependent. But because little more is known about t, it is not possible to carry out more than the simple single scattering, impulse approximation to the hypernucleus production rates. In the region 500 - 800 MeV/c., the sum was truncated at $n=2$ because of the difficulty in defining the other coefficients. If the cross sections where measured more carefully at many angles then it would be possible, in the framework of the model presented here, to put all the experimental information into the calculation. However this has not been done and would not be a significant improvement considering many other effects are more important and will also be neglected like nuclear distortion, spin-orbit splitting and multiple scattering effects.

Chapter 3 Nuclear Wave Function

For the purpose of this work, only doubly magic (N = Z) nuclei will be considered and the choice for a model wave function of the nucleus will be based on the physical process we have under consideration. For example, suppose that a deep one hole state is created in the final hypernucleus, say $(1s)^{-1}_{1/2}$ in ^{16}O , then the system will be in a very highly excited state and will have many fast decay channels with lifetimes much shorter than the lambda's lifetime in the nucleus. Processes, like the aforementioned, are interesting in their own right but reactions where the final hypernucleus has a small percentage of the available energy are more likely to form "stable" hypernuclei. Therefore, it is reasonable to take the interaction between the incident kaon and the nucleus to be one with only those nucleons on the top of the nuclear fermi sea. For example, in the case of ^{16}O it is assumed that we have an inert helium core on which we build an anti-symmetric state of 6 protons and 6 neutrons. To describe the nucleons near the top of the fermi sea, independent particle wave functions, with spin and isospin, are used in an L-S coupling scheme, neglecting the spin - orbit interactions. The average nuclear potential is taken to be given by a harmonic oscillator with an experimentally determined oscillator strength (Harmonic oscillator wave functions are used because of the facility for expressing the cross sections in a closed form).

The single particle wave functions are denoted $\phi_n(l, s, t, m_l, m_s, m_t)$ or simply $\phi_n(\alpha)$, where n is the radial total quantum number, l, s, t, are the orbital, spin and isospin quantum numbers and m_l, m_s, m_t, are the z-components of l, s, t respectively.

Since it has been assumed that only two body interactions are important for the K-Nucleus interaction, it is useful to factorize the target wave function into one for a single nucleon times a wave function for the remaining nucleons, summed over possible single particle states. This factorization is the well known fractional parentage expansion (Elliott, J.P. and Lane, A.M., 1957).

To conclude this section the method of fractional parentage expansions is sketched in order to establish notation. (McCarthy, I.E., 1968) If the anti-symmetric state of A nucleons in the configuration $(\ell)^A$ is denoted by $\chi^A(\ell^A, \alpha_A)$ where $\alpha_A = (L_A, S_A, T_A, m_{L_A}, m_{S_A}, m_{T_A})$ and the anti-symmetric state of A-1 nucleons in the configuration $(\ell)^{A-1}$ by $\chi^{A-1}(\ell^{A-1}, \alpha_{A-1})$ then it is possible to write

$$\chi^A(\ell^A, \alpha_A) = \sum_{\phi_n^A} \langle \chi^A \{| \chi^{A-1}\phi_n^A \rangle \{ \chi^{A-1}(\ell^{A-1}, \alpha_{A-1})\, \phi_n^A(\alpha) \}^{\alpha_A} \tag{9}$$

where $\phi_n^A(\alpha)$ is the single particle state of the Ath nucleon and $\langle \{| \rangle$ is the one-particle fractional parentage coefficient. The summation extends over all possible states $\phi_n^A(\alpha)$ allowed to the Ath nucleon. Finally $\{ , \}^{\alpha_A}$ denotes the vector coupling of the Ath particle to the state of the A-1 nucleons to give the quantum numbers of the total wave function of the A nucleons. In the case when spin-orbit interactions are neglected one has;

$$\begin{aligned} \{ \chi^{A-1}, \phi^A \}^{\alpha_A} = \sum_{\substack{m_\ell, m_s, m_t \\ L_A, S_A}} & (L_{A-1}\, \ell\, m_{L_{A-1}}\, m_\ell \,|\, L_A m_{L_A})(S_{A-1}\, s\, m_{S_{A-1}}\, m_s \,|\, S_A m_{S_A}) \\ & \times (T_{A-1}\, t\, m_{T_{A-1}}\, m_t \,|\, T_A m_{T_A})(L_A\, m_{L_A}\, S_A\, m_{S_A} \,|\, J_A m_{J_A}) \\ & \times \chi^{A-1}(\ell^{A-1}, \alpha_{A-1})\, \phi_n^A(\ell\, s\, t\, m_\ell\, m_s\, m_t) \end{aligned} \tag{10}$$

The fractional parentage coefficients are determined by requiring $\langle \{| \rangle$ to be anti-symmetric and normalized to unity. The coefficients such as $(L_{A-1}\, \ell\, m_{L_{A-1}}\, m_\ell \,|\, L_A m_{L_A})$ are Clebsch-Gordan coefficients.

For conciseness Eq. (9) will be abbreviated

(11) $$\chi^{A} = \sum c_{\alpha_A,\alpha_{A-1}} \chi^{A-1} \phi_n^A(\alpha)$$

with

$$c_{\alpha_A,\alpha_{A-1}} = \langle \chi^A \{ | \chi^{A-1} \phi_n^A(\alpha) \rangle (L_{A-1}\, \ell\, m_{L_{A-1}}\, m_\ell \,|\, L_A\, m_A) \times$$
$$(S_{A-1}\, s\, m_{S_{A-1}}\, m_s \,|\, S_A\, m_{S_A}) (L_A\, S_A\, m_{L_A}\, m_{S_A} \,|\, J_A\, m_{T_A}) \times$$
$$(T_{A-1}\, t\, m_{T_{A-1}}\, m_t \,|\, T_A\, m_{T_A})$$

and the summation extending over $\phi_n^A(\alpha)$, m_ℓ, m_s and m_t.

In a similiar way the wave function of the final hypernucleus is expressible as the lambda wave function coupled to the A-1 nucleon system to give a final state with the total quantum numbers of final hypernucleus:

(12) $$\chi^{A-1}(\ell'^{A-1}, \alpha'_{A-1}, \Lambda) = \sum c^{\Lambda}_{\alpha'_{A-1},\alpha_{A-1}} \chi^{A-1}(\ell'^{A-1}, \alpha_{A-1})\, \eta_n^{\Lambda}(\ell_\Lambda s_\Lambda m_{\ell_\Lambda} m_{s_\Lambda}) .$$

The fractional parentage coefficient contained in $c^{\Lambda}_{\alpha'_{A-1},\alpha_{A-1}}$ is unity since the hypernucleus must only be anti-symmetric with respect to the A-1 nucleons, not the total Λ-(A-1) nuclear system.

Chapter 4 Differential Cross section

The initial state of the K^--Nucleus system will be given by the product of the meson wave function and the nuclear state in the overall center of mass;

$$|\psi_i\rangle = |\underset{\sim}{k}_K\rangle_K \, |-\underset{\sim}{k}_K\rangle_A \, |\chi^A(\ell^A, \alpha_A)\rangle \tag{13}$$

where $\underset{\sim}{k}_K$ is the momentum of the kaon in the overall center of mass(O.C.M.). The wave function of the nucleus is the product of the internal wave function $|\chi^A(\ell^A, \alpha_A)\rangle$ and the motion of the center of mass of the nucleus, described by the plane wave $|-\underset{\sim}{k}_K\rangle_A$. If $\underset{\sim}{r}_K$ and $\underset{\sim}{R}$ are the coordinates of the kaon and nucleus in the O.C.M. the plane wave states are given by

$$\begin{aligned} \langle \underset{\sim}{r}_K | \underset{\sim}{k}_K\rangle_K &= \sqrt{2\omega_K}\ \exp(i\,\underset{\sim}{k}_K\cdot\underset{\sim}{r}_K) \\ \langle \underset{\sim}{R} | -\underset{\sim}{k}_K\rangle_A &= \sqrt{2\omega_A}\ \exp(-i\,\underset{\sim}{k}_K\cdot\underset{\sim}{R}) \end{aligned} \tag{14}$$

and where ω_K and ω_A are the relativistic energies of the kaon and nucleus respectively. The normalization used here is the same as that used in the parametrization of the transition amplitude for $n(K^-,\pi^-)\Lambda$ given in Chapter 2 (Källén, G., 1964; Martin, A.D., Spearman, T.D., 1970) in defining $\mathcal{T}$.

Similarly the final state will be the product of an outgoing pion state and the hypernucleus wave function;

$$|\psi_f\rangle = |\underset{\sim}{k}_\pi\rangle_\pi \, |-\underset{\sim}{k}_\pi\rangle_{A_\Lambda} \, |\chi^{A-1}(\ell^{A-1}, \alpha_{A-1}, \Lambda)\rangle \tag{15}$$

with $\underset{\sim}{k}_\pi$ the O.C.M. momentum of the outgoing pion.

Because the cross sections we are describing involve the initial struck nucleon and the final lambda both in bound states, it is necessary to know their wave functions in momentum space relative to the residual A-1 nucleons. If $\underset{\sim}{r}$ is the position of the nucleon relative to the center of mass of the A nucleon system, the wave function in momentum space is given by

$$\phi_n(\underset{\sim}{k}) = \frac{1}{(2\pi)^{3/2}} \int d\underset{\sim}{r}\, \exp(i\underset{\sim}{k}\cdot\underset{\sim}{r})\, \phi_n(\underset{\sim}{r}) \tag{16}$$

where $\underset{\sim}{k}$ is the momentum of the nucleon relative to the center of mass of the nucleus. A similar expression holds for the bound lambda's wave function.

In order to find the momentum of the neutron relative to the A-1 nucleons, consider Fig. 4. If $\underset{\sim}{r}_n$ is the coordinate of the nucleon relative to the O.C.M., $\underset{\sim}{R}$ the center of mass of the nucleus and $\underset{\sim}{r}_p$ of the A-1 nucleon system, then the momentum conjugate to $\underset{\sim}{r} = \underset{\sim}{r}_n - \underset{\sim}{r}_p$ is

$$\underset{\sim}{k}_r = \frac{m_p \underset{\sim}{k}_n - m_n \underset{\sim}{k}_p}{m_A} \tag{17}$$

and in the O.C.M., $\underset{\sim}{k}_R = \underset{\sim}{k}_n + \underset{\sim}{k}_p = -\underset{\sim}{k}_K$.

From these results the momenta of the nucleon and the residual nucleus in the O.C.M. are given by;

$$\begin{aligned} \underset{\sim}{k}_n &= \underset{\sim}{k}_r - \frac{m_n}{m_A}\underset{\sim}{k}_K \\ \underset{\sim}{k}_p &= -\underset{\sim}{k}_r - \frac{m_p}{m_A}\underset{\sim}{k}_K \end{aligned} \tag{18}$$

Because single particle wave functions will be used to describe both the nucleon and the lambda, it is necessary to relate the wave functions which are defined with respect to the center of mass of the nucleus to wave functions expressed in terms of the separation between the nucleon (lambda) and the C.M. of the A-1 nucleon system. The separation between the nucleon and the nucleus center of mass is given by

$$\underset{\sim}{r} = \frac{m_p}{m_A}\underset{\sim}{r} \tag{19}$$

It is $\underset{\sim}{r}$ which is used in the description of the single particle wave function.

The initial state of the nucleus is given by

$$(20)\quad \langle \underset{\sim}{r}\,\underset{\sim}{R} | \chi^A \rangle = \sqrt{2\omega_A}\, \exp(-i\underset{\sim}{k}_K\cdot\underset{\sim}{R}) \sum C_{\alpha_A,\alpha_{A-1}}\, \phi_n(\underset{\sim}{r},\alpha)\, \chi^{A-1}(\ell^{A-1},\alpha_{A-1}) \;.$$

Using Eq. (16) one finds

$$(22)\quad \langle \underset{\sim}{r}\,\underset{\sim}{R} | \chi^A \rangle = \sqrt{2\omega_A} \sum C_{\alpha_A,\alpha_{A-1}} \int \frac{d\underset{\sim}{k}'}{(2\pi)^{3/2}}\, \phi_n(\underset{\sim}{k}',\alpha)\, \exp(i\underset{\sim}{k}'\cdot\underset{\sim}{r} - i\underset{\sim}{k}_K\cdot\underset{\sim}{R})\, \chi^{A-1} \;.$$

However it is simple to show that

$$(23)\qquad \underset{\sim}{k}'\cdot\underset{\sim}{r} - \underset{\sim}{k}_K\cdot\underset{\sim}{R} \equiv \underset{\sim}{k}_n\cdot\underset{\sim}{r}_n + \underset{\sim}{k}_p\cdot\underset{\sim}{r}_p$$

with

$$k_n = \frac{m_p}{m_A}\underset{\sim}{k}' - \frac{m_n}{m_A}\underset{\sim}{k}_K$$

$$k_p = \frac{-m_p}{m_A}(\underset{\sim}{k}' + \underset{\sim}{k}_K) \;.$$

Then the initial wave function becomes

$$(24)\quad \langle \underset{\sim}{r}_n\,\underset{\sim}{r}_p | \chi^A \rangle = \sqrt{2\omega_A} \sum C_{\alpha_A,\alpha_{A-1}} \int \frac{d\underset{\sim}{k}'}{(2\pi)^{3/2}}\, \phi_n(\underset{\sim}{k}',\alpha)\, \exp(i\underset{\sim}{k}_n\cdot\underset{\sim}{r}_n)\, \exp(i\underset{\sim}{k}_p\cdot\underset{\sim}{r}_p)\, \chi^{A-1} \;.$$

Similar expressions hold for the final state lambda-pion system.

As remarked earlier, the choice of plane wave normalization was related to the definition for the transition amplitude of the process $n(K^-,\pi^-)\Lambda$. Consider Eq. (24), it is clear that one can interpret the exponentials as plane waves for the nucleon and the residual nucleus if normalization factors are introduced. The initial nuclear wave function is then given by

$$(25)\quad |\chi^A\rangle = \sqrt{\frac{\omega_A}{2\omega_n\omega_p}} \sum C_{\alpha_A,\alpha_{A-1}} \int \frac{d\underset{\sim}{k}'}{(2\pi)^{3/2}}\, \phi_n(\underset{\sim}{k}',\alpha)\, |\underset{\sim}{k}_n\rangle\, |\underset{\sim}{k}_p\rangle\, |\chi^{A-1}\rangle \;.$$

Similiarly the final hypernucleus wave function is

$$(26)\qquad |\chi^{A-1}_{\Lambda}\rangle = \sqrt{\frac{\omega_{A_\Lambda}}{2\omega_\Lambda \omega_p}} \sum C^{\Lambda}_{\alpha'_{A-1},\alpha_{A-1}} \int \frac{d\underset{\sim}{k}}{(2\pi)^{3/2}} \eta^{\Lambda}_{n}(\underset{\sim}{k}) |\underset{\sim}{k}_\Lambda\rangle |\underset{\sim}{k}_{p'}\rangle |\chi^{A-1}\rangle \;,$$

Using these expressions the transition operator for the reaction $K^- +$ nucleus $\rightarrow \pi^- +$ hypernucleus is given by

$$T_{fi} = N\left(\frac{\omega_{A_\Lambda}\omega_A}{\omega_\Lambda \omega_n}\right)^{1/2}\left(\frac{m_{A^\Lambda}}{m_p}\right)^3 \sum_{\substack{m_\ell, m_s, m_\pi \\ m_{\ell_\Lambda}, m_{s_\Lambda}}} C^{\Lambda\,*}_{\alpha'_{A-1},\alpha'_{A-1}} C_{\alpha_A,\alpha_{A-1}} \langle \chi^{A-1'} | \chi^{A-1}\rangle$$

$$(27)\qquad \times \int d\underset{\sim}{k}' \, \eta^{\Lambda\,*}_{n_\Lambda \ell_\Lambda s_\Lambda m_{\ell_\Lambda} m_{s_\Lambda}}(\underset{\sim}{k})\, \phi_n(\underset{\sim}{k}',\alpha) \langle \underset{\sim}{k}_\pi \underset{\sim}{k}_\Lambda | t | \underset{\sim}{k}_K \underset{\sim}{k}_n\rangle \;.$$

where N is the number of identical scatterers and

$$\underset{\sim}{k} = \left(\frac{m_{A^\Lambda}}{m_A}\right)(\underset{\sim}{k}_K + \underset{\sim}{k}') - \underset{\sim}{k}_\pi \;.$$

Finally if we assume the initial and final residual nuclei are unaffected by the reaction, so that $\langle \chi^{A-1'} | \chi^{A-1}\rangle = \delta_{p'p}$, then the total transition amplitude is

$$T_{fi} = N\left(\frac{\omega_{A_\Lambda}\omega_A}{\omega_\Lambda \omega_n}\right)^{1/2}\left(\frac{m_{A_\Lambda}}{m_p}\right)^3 \sum C^{\Lambda\,*}_{\alpha_{A-1}\alpha_{A-1}} C_{\alpha_A,\alpha_{A-1}}$$

$$(28)\qquad \times \int d\underset{\sim}{k}' \, \eta^{\Lambda\,*}_{n_\Lambda \ell_\Lambda s_\Lambda m_{\ell_\Lambda} m_{s_\Lambda}}(\underset{\sim}{k})\, \phi_n(\underset{\sim}{k}',\alpha) \langle \underset{\sim}{k}_\pi \underset{\sim}{k}_\Lambda | t | \underset{\sim}{k}_K \underset{\sim}{k}_n\rangle \;.$$

By making this assumption, we assume that there is no nuclear deformation in the reaction and hence, the nucleus only plays a kinematical role and acts as a source of scatterers. Fortunately, if we are only interested in doubly magic nuclei like helium, carbon and oxygen, then the fractional one particle parentage coefficients are equal, hence $|\langle \,\}\, | \,\rangle| = 1/\sqrt{N}$, because they are normalized to unity, and

$$(29)\qquad C_{\alpha_A,\alpha_{A-1}} = \frac{(\text{phase})}{\sqrt{N}} \times (\text{Clebsch-Gordan coefficients}) \,.\,.$$

The transition amplitude is then given by

$$T_{fi} = \sqrt{N}\left(\frac{\omega_{A_\Lambda}\omega_A}{\omega_\Lambda\omega_n}\right)^{1/2}\left(\frac{M_A^\Lambda}{M_p}\right)^3 \sum C^{\Lambda\,*}_{\alpha_{A-1},\alpha_{A-1}}\, C'_{\alpha_A,\alpha_{A-1}}$$

$$(30) \qquad \times \int d\underset{\sim}{k}'\; \eta^{\Lambda\,*}_{n_\Lambda \ell_\Lambda s_\Lambda m_{\ell_\Lambda} m_{s_\Lambda}}(\underset{\sim}{k})\,\phi_n(\underset{\sim}{k}',\alpha)\,\langle \underset{\sim}{k}_\pi \underset{\sim}{k}_\Lambda | t | \underset{\sim}{k}_K \underset{\sim}{k}_n\rangle$$

$$C^{\Lambda}_{\alpha_{A-1},\alpha_{A-1}}\, C'_{\alpha_A,\alpha_{A-1}} = (L_p\, \ell_\Lambda\, m_{L_p} m_{\ell_\Lambda} | L_f m_{L_f})(L_p\, \ell\, m_{L_p} -m_{L_p}|00)$$
$$\times\ (S_p\, s_\Lambda\, m_{s_p} m_{s_p} | S_f m_{S_f})(S_p\, s\, m_{s_p} -m_{s_p}|00)$$
$$\times\ (T_p\, t\, m_{T_p} -m_{T_p}|00)\ (L_f\, S_f\, m_{L_f} m_{s_f} | J_f m_f)$$

where we have used the fact that the initial nucleus has $L_i = S_i = T_i = 0$. In Appendix 2 the factor $\sqrt{N}$ times the amplitude is explained in terms of Slater determinants.

The integral in Eq. (30) is rather complicated and so it is desirable to replace it be some convenient approximation. Because of the use of harmonic oscillator wave functions, the integral will be dominated by small momenta and will have vanishing contributions for large $\underset{\sim}{k}'$.. Similarly $\langle \pi\Lambda | t | K n\rangle$ will not be a strong function of $\underset{\sim}{k}'$ for small $\underset{\sim}{k}'$. Hence as a first approximation to the integral in Eq. (30), $\langle \underset{\sim}{k}_\pi \underset{\sim}{k}_\Lambda | t | \underset{\sim}{k}_K \underset{\sim}{k}_n\rangle$ is replaced by its value when $\underset{\sim}{k}'=0$. The total transition amplitude may henceforth be written as:

$$(31) \qquad T_{fi} = \sqrt{N}\left(\frac{\omega_{A_\Lambda}\omega_A}{\omega_\Lambda\omega_n}\right)^{1/2} \langle \pi\Lambda | t | K n\rangle_{\underset{\sim}{k}'=0}\, \mathcal{F}_{fi}(\underset{\sim}{q})$$

with $\langle \pi\Lambda | t | K n\rangle_{\underset{\sim}{k}'=0}$ to be evaluated in the K-nucleus center of mass. This is now a high energy approximation to the total transition amplitude, that neglects most of the nuclear effects and puts the major structural effects into the inelastic form factor $\mathcal{F}_{fi}$, where $\mathcal{F}_{fi}(\underset{\sim}{q})$ has been defined as

$$(32) \qquad \mathcal{F}_{fi} = \left(\frac{m_{A_\Lambda}}{m_p}\right)^3 \sum C^{\Lambda *}_{\alpha_{\Lambda-1}\alpha_{\Lambda-1}} C'_{\alpha_\Lambda, \alpha_{\Lambda-1}} \int d\underset{\sim}{k}' \, \eta^*_{\ell_\Lambda s_\Lambda m_{\ell_\Lambda} m_{s_\Lambda}}(\underset{\sim}{k}) \, \phi_n(\underset{\sim}{k}', \alpha)$$

$$\underset{\sim}{q} = \left(\frac{m_{A_\Lambda}}{m_A}\right) \underset{\sim}{k}_K - \underset{\sim}{k}_\pi \quad .$$

Here $-\underset{\sim}{q}$ is the three momentum transfer. When $m_{A_\Lambda} \to m_A$ it reduces to the momentum transfer for elastic scattering.

The differential cross section is then given by (Källén, G., 1964),

$$(33) \quad \left(\frac{d\sigma}{d\Omega}\right) = \frac{N}{64\pi^2 S} \left(\frac{\omega_{A_\Lambda} \omega_A}{\omega_n \omega_A}\right) \sqrt{\frac{\lambda(S, m_{A_\Lambda}^2, m_\pi^2)}{\lambda(S, m_A^2, m_K^2)}} \; |t|^2 \left(\sum_f |\mathcal{F}_{fi}(\underset{\sim}{q})|^2\right) .$$

S is the total energy squared.

Chapter 5 Applications

(a) Helium

In the reaction $^4He(K^-,\pi^-)^4He_\Lambda$, the production of the lambda-hyperon occurs with a neutron in a (1s) state in the nucleus. The hypernucleus $^4He_\Lambda$ has only one state in which the binding energy is positive and this state has the shell model configuration $(1s)_n^{-1}(1s)_\Lambda$, - both the nucleon and the bound lambda are in states of zero angular momentum relative to the center of mass of the hypernucleus. The parent or residual nuclear system ^3He, has the quantum numbers $L_p=0$, $S_p=\frac{1}{2}$, $T_p=\frac{1}{2}$ and $m_{t_p}=+\frac{1}{2}$. The bound lambda hyperon has the quantum numbers $l=0$, $s=\frac{1}{2}$ and $t=0$. Because the interaction contains no spin-flip terms, the bound lambda must have the same spin quantum numbers as the struck neutron. That is, the total spin (spin is a good quantum number in our model) of the hypernucleus $^4He_\Lambda$ must be identically zero.

Three dimensional harmonic oscillator wave functions are used to describe both the struck neutron and the bound lambda. The radial wave functions are given by

$$R_{1s}(r) = \left(\frac{4}{\sqrt{\pi}\,a_n^3}\right)^{1/2} \exp(-r^2/2a_n^2)$$

(34)

$$R_{1s}^\Lambda(r) = \left(\frac{4}{\sqrt{\pi}\,a_\Lambda^3}\right)^{1/2} \exp(-r^2/2a_\Lambda^2)$$

with the oscillator strength a_n and a_Λ for the nucleon and lambda respectively. The value of a_n is well known from electron scattering and has the value 1.38fm. The value of a_Λ for this form of the lambda wave function is not well defined. This is basically because the Gaussian form for the wave function is not a very good description of the lambda hyperon s-state in $^4He_\Lambda$. In order to assign a value to a_Λ for our calculations, the nonrelativistic Schrodinger equation was integrated numerically for a Woods-Saxon potential of range 2.0 fm. and diffuseness 0.6 fm., given that the lambda in $^4He_\Lambda$ has a binding energy of 2.25 MeV. The resulting wave function is shown in figure 5. The wave function is seen to peak just inside the well radius. In order to fit this curve with a Gaussian form, one must take an oscillator strength a_Λ=1.90 fm. approximately. This was the value used in all the calculations that are reported here.

The inelastic form factor $\mathcal{F}_{fi}$ was calculated using the above wave functions and is given by

(35) $$\mathcal{F}(q^2) = \frac{1}{\sqrt{2}} \left(\frac{m_{^4He_\Lambda}}{m_{^4He}} \right)^3 \left(\frac{a'^2}{a_n^3 a_\Lambda^3} \right)^{1/2} \exp\left(-a'^2 q^2/4\right)$$

with $$\frac{1}{a'^2} = \frac{1}{2a_n^2} + \left(\frac{m_{^4He_\Lambda}}{m_{^4He}} \right) \frac{1}{2a_\Lambda^2}$$

and $$q = \left(\frac{m_{^4He_\Lambda}}{m_{^4He}} \right) \underset{\sim}{k}_\pi - \underset{\sim}{k}_K .$$

The differential cross section for production of $^4He_\Lambda$ is

(36) $$\left(\frac{d\sigma}{d\Omega} \right)_{c.m.} = \frac{4}{64\pi^2 s} \left| \frac{\underset{\sim}{k}_\pi}{\underset{\sim}{k}_K} \right| \left(\frac{\omega_{^4He_\Lambda} \omega_{^4He}}{\omega_n \omega_\Lambda} \right) |\langle \pi\Lambda | t | Kn \rangle|^2 \, |\mathcal{F}(q^2)| .$$

At forward angles, where the momentum transfer will be small, the inelastic form factor will be maximum. Figures (6,7) show $(d\sigma/d\Omega)_{c.m.}$ as a function of the incident kaon laboratory momentum and as a function of the scattering angle in the center of mass. The rapid drop in the calculated cross sections as a function of angle illustrate the large momentum transfer encountered as one goes to larger scattering angles. The slope of the curves is a measure of the value of a'^2, which is a direct measure of the value of a_Λ taken in our calculations.

(b) Carbon

The production of $^{12}C_\Lambda$ is the production of a "p-shell hypernucleus", (p-shell refers to the nuclear shell of the struck nucleon, not the Λ wave function). These have been discussed in some detail (Gal, A., Soper, J.M., Dalitz, R.H., 1971). In the calculations we have performed, it is the p-shell nucleons which are responsible for the production of the hypernucleus. The s-shell nucleons remain inert throught the reaction. The residual nucleus which couples to the lambda-hyperon wave function can then be considered to be $(1p)^{-1}_n$ hole state, with $L_p = 1, S_p = \frac{1}{2}, T_p = \frac{1}{2}$ and $m_{T_p} = 1/2$. In p-shell hypernuclei there is also the possibility of states other than the lambda in a s-state which may be bound. In our calculations, we have taken both the s-state and the p-state of the Λ-hyperon as "bound" by 10.0 MeV. and .5 MeV. respectively. One word concerning the p-states of the lambda which we have considered bound. Experimentally and theoretically, it is not clear whether some, all or none of these states will be bound. Hence our calculations concerning the p-states of the lambda actually mean that if all the p-states $(1p)^{-1}_{1/2}(1p)^{\Lambda}_{1/2}$, $(1p)^{-1}_{3/2}(1p)^{\Lambda}_{1/2}$, $(1p)^{-1}_{3/2}(1p)^{\Lambda}_{3/2}$, $(1p)^{-1}_{1/2}(1p)^{\Lambda}_{3/2}$ are degenerate and bound by 0.5 MeV., then one should expect p-state cross sections of the approximate size and shape predicted by our calculations. Clearly, our results should therefore be taken with a grain of salt and considered very speculative. Again because there is no spin flip involved in reaction (1) in our model, the final spin of the hypernucleus is taken as zero. The final states of the hypernucleus are then $L_f = 2,1,0, S_f = 0, T_f = \frac{1}{2}$. The radial wave function of the struck nucleon is

(37) $$R_{1p}(r) = \left(\frac{8}{3\sqrt{\pi}\, a_n^3}\right)^{1/2} \frac{r}{a_n} \exp\left(-r^2/2a_n^2\right)$$

with a_n the measured value 1.56 fm. from electron scattering data. For the final state of the lambda in a s-state, the radial wave function is given by

$$R_{1s}^{\Lambda}(r) = \left(\frac{4}{\sqrt{\pi}\, a_\Lambda^3}\right)^{1/2} \exp\left(-r^2/2a_\Lambda^2\right) \quad . \tag{38}$$

For p-shell hypernuclei it is found that $a_\Lambda = 1.74$ fm. gives a reasonably good fit to the calculated wave function (Gal, A., Soper, J.M., and Dalitz, R.H., 1971). In this case, the final state produced is $(1p)_n^{-1}(1s)_\Lambda$ and the inelastic form factor becomes

$$\mathcal{F}(q^2) = \frac{i}{\sqrt{6}} \left(\frac{a'^8}{a_\Lambda^3 a_n^5}\right)^{1/2} \left(\frac{m_{^{12}C_\Lambda}}{m_{^{12}C}}\right)^3 a' q \exp\left(-a'^2 q^2/4\right) \quad . \tag{39}$$

where
$$\frac{1}{a'^2} = \frac{1}{2a_n^2} + \left(\frac{m_{^{12}C}}{m_{^{12}C_\Lambda}}\right)^3 \frac{1}{2a_\Lambda^2}$$

and
$$\underset{\sim}{q} = \left(\frac{m_{^{12}C_\Lambda}}{m_{C^{12}}}\right) \underset{\sim}{k_\pi} - \underset{\sim}{k_K} \quad .$$

The differential cross section for the production of the state is then given by

$$\frac{d\sigma}{d\Omega} = \frac{8}{64\pi^2 s} \left|\frac{\underset{\sim}{k_\pi}}{\underset{\sim}{k_K}}\right| \left(\frac{\omega_{^{12}C}\,\omega_{^{12}C_\Lambda}}{\omega_n\,\omega_\Lambda}\right) |\langle \pi\Lambda|t|Kn\rangle|^2_{t'=0}$$
$$\times \frac{1}{6} \left(\frac{m_{^{12}C_\Lambda}}{m_{^{12}C}}\right)^6 \left(\frac{a'^8}{a_\Lambda^3 a_n^5}\right) a'^2 q^2 \exp\left(-a'^2 q^2/2\right) \quad . \tag{40}$$

The differential cross sections are plotted in Figures (8,9,10,11)(curve a) as functions of the cosine of the scattering angle in the kaon-nucleus center of mass. At forward angles the cross section vanishes because $q^2 \to 0$ but it rises to an appreciable value for $\cos \Theta_{c.m.} = .95$. At these angles, the production of the state $(1p)_n^{-1}(1s)_\Lambda$ is seen to be an appreciable part of any reasonable estimates for the total differential cross section for Λ production summed over all possible final states.

For the production of the lambda-hyperon in a bound p-state the lambda wave function was integrated for a Wood-Saxon potential of range 2.6 fm., diffuseness 0.5 fm. taking the Λ to be bound by only 0.5 MeV. The wave function is plotted in figure (12). It peaks at $r = 2.50$ and for a 3-dimensional harmonic oscillator fit, this implies that the approximate oscillator strength is 1.76 fm. This value is in very close agreement with that used by Gal et al for the lambda in s-states (for models of hypernuclei, see Iwao, S., 1971; Shakin, C.H., et al, 1967). The hypernucleus state will then be $(1p)_n^{-1}(1p)_\Lambda$ which will have the possibility of $L_f = 2,1,0$. The sum over these states, gives an inelastic form factor squared,

$$(41)\quad \sum |\mathcal{F}_{fi}(q^2)|^2 = \frac{1}{2}\left(\frac{m_{^{12}C_\Lambda}}{m_{^{12}C}}\right)^6\left(\frac{2a_\Lambda a_n}{a_\Lambda^2+a_n^2}\right)^5\left\{1-\frac{1}{3}a'^2q^2+\frac{1}{12}a'^4q^4\right\}\exp\left(-\frac{a'^2q^2}{2}\right)$$

when the radial wave function of the lambda is given by

$$(42)\qquad R_{1p}^{\Lambda}(r) = \left(\frac{8}{3\sqrt{\pi}\,a_\Lambda^3}\right)\frac{r}{a_\Lambda}\exp\left(-\frac{r^2}{2a_\Lambda^2}\right)$$

Thus the differential cross section for the production of the hypernucleus state $(1p)_n^{-1}(1p)_\Lambda$ is given by

$$(43)\quad \frac{d\sigma}{d\Omega} = \frac{8}{64\pi^2 S}\cdot\frac{|\underset{\sim}{k}_\pi|}{|\underset{\sim}{k}_K|}\cdot\left(\frac{\omega_{^{12}C}\,\omega_{^{12}C_\Lambda}}{\omega_n\,\omega_\Lambda}\right)\left(\frac{m_{^{12}C_\Lambda}}{m_{^{12}C}}\right)^6 |\langle\pi\Lambda|t|Kn\rangle|^2_{\underset{\sim}{t}'=0}$$

$$\times\frac{1}{2}\left(\frac{2a_n a_\Lambda}{a_\Lambda^2+a_n^2}\right)^5\left\{1-\frac{1}{3}a'^2q^2+\frac{1}{12}a'^4q^4\right\}\exp\left(-\frac{a'^2q^2}{2}\right).$$

As $q^2\to 0$, this differential cross section has a maximum. This corresponds roughly to changing the struck neutron into a lambda without any momentum transfer and without changing the spatial distribution of the system by a great deal. Notice that as $a_\Lambda \to a_n$, and $q^2 \to 0$ that this differential cross section would tend to $\sim 4 \times (d\sigma/d\Omega)$free. This corresponds to the case in which the struck neutron and bound lambda have exactly the same spatial distribution and inelastic form factor becomes a quasi-elastic form factor which is unity for zero momentum transfer. The differential cross sections are plotted in Figures 8,9,10,11, (curve b) for the production of the $(1p)_\Lambda$ states, at incident kaon momenta of 500, 600, 700, and 800 MeV/c.

The apparent dip in the cross section comes from the state $(1p)^{-1}_n(1p)_\Lambda$ coupled to zero angular momentum. When $a^2q^2 \simeq 6$, this term becomes zero, in analogy with elastic form factor from electron scattering. It is the contribution from $L_f=2$ which fills in the gap in this region (see momentum transfer graphs 18,19).

(c) Oxygen

The calculations for oxygen follow exactly the same pattern as for carbon. In order to find a value for the oscillator strength for the p-state in $^{16}O_\Lambda$, the Schrodinger equation was integrated for Woods-Saxon well of radius 2.90 fm., diffuseness 0.6 fm. and with binding energy of 1.0 MeV. The wave function is plotted in Fig. 13. An appropriate oscillator fit gives an oscillator strength of a_Λ = 1.91 fm. This is the value used in our calculations. The only other trivial changes from carbon to oxygen are, the effective number of scatters and the kinematical changes. The oscillator strength for the nucleons was taken as 1.56 fm.

In Figs. (14,15,16,17) the differential cross sections for both s and p state production are presented for various incident kaon momenta. These results have the same structure as the carbon results.

Chapter 6 Conclusion and Discussion

(a) General Comments

The first and most obvious comment is that the differential cross sections are strongly momentum dependent. This occurs from two sources; the inelastic form factors $\mathcal{F}(q^2)$ and from the behaviour of $(d\sigma/d\Omega)$ free in the lab. At high incident kaon momenta, the momentum transfer is large everywhere except in a very narrow cone around the zero scattering angle. As a result of the rapid increase in $|q|$ with angle, all the differential cross sections are strongly peaked toward forward scattering angles.

One of the most important parameters in the model we have presented is a_Λ , the parameter which determines the spatial wave function of the lambda hyperon. In all the model calculations we have presented, these oscillator parameters where choosen with some care. Either the existing values in the literature where used or in cases of uncertainty, the wave equation was integrated numerical and fitted by eye to an appropriate oscillator value. The final results are very sensitive to its choice and can vary by as much as a factor of 2. As an example, in the production of the hypernucleus state $(1p)_n^{-1}(1p)_\Lambda\,{}^{16}O_\Lambda$, the square of inelastic form factor is proportional to $2a_\Lambda a_n/(a_\Lambda^2+a_n^2)$ to the fifth power. When $a_\Lambda=a_n$, this factor is unity but in the actual case of ^{16}O this factor to fifth power is .73 . As a_Λ is made larger or smaller than a_n, this factor decreases from its maximum value of 1. a_Λ also determines the peak in the differential cross section for the state $(1p)_n^{-1}(1s)_\Lambda$ through a'^2. Changes in a_Λ , move the peak outward when $a_n > a_\Lambda$ and inward when $a_\Lambda < a_n$. Thus the predicted cross sections are indeed sensitive to a_Λ .

Finally, throughout the calculations, the kinematics where treated relativistically. Only the motion of the nucleons and bound Λ where treated non-relativistically. Also, when the dependence on $\underset{\sim}{k}'$ in 大 was ignored, this assumption neglected the fact that the interaction actually occurs in a nuclear potential. This means that the reaction $n(K^-,\pi^-)\Lambda$ proceeds at a slightly higher energy than was assumed in the calculations by an amount equal to the depth of the average potential well for the lambda. These off-shell affects, should not be significant however for the high momentum cases studied in this work.

(b) Experimental Consequences

The results we have predicted mean little until we ask what are the experimental consequences, if any of our results.

The model we have used is rather simple, lacking in many fine details but the essential features of the calculations are significant. The calculations concerning the p-shell hypernuclei are the most interesting, because it is here that the possibility of excited hypernuclear states exist and the possibility of being able to study them intriguing to the experimentalists.

In this section, we shall confine ourselves to discussions related to $^{16}O_\Lambda$. What is said is equally true for $^{12}C_\Lambda$. In our calculations of O^{16}_Λ the Λ was taken as bound by 10.0 MeV. in it's relative 1s state and by 1.0 MeV. in it's relative 1p state. But in point of fact this is an extreme simplification there are two 1s states, $(1p)^{-1}_{3/2}(1s)_\Lambda$ and $(1p)^{-1}_{1/2}(1s)_\Lambda$ separated by roughly 6 Mev. (Ajzenberg-Selove, F., 1970). These states are again split by the spin-spin interaction into 4 states, each separated by approximately 1 MeV. No evidence for the existence of the p-state exists. If it did however, it would in point of fact be the following states $(1p)^{-1}_{3/2}(1p)^{\Lambda}_{1/2}$, $(1p)^{-1}_{3/2}(1p)^{\Lambda}_{3/2}$, $(1p)^{-1}_{1/2}(1p)^{\Lambda}_{1/2}$ and $(1p)^{-1}_{1/2}(1p)^{\Lambda}_{3/2}$ a total of 4 different configurations, with total of 8 different states, when spin-spin forces are taken into account. Many of these states will be unbound and some will probably be just slightly bound. No one knows how many will be bound, if any, and the hope is that experiments may be able to see these states if background is not high.

The experimental missing mass plot, assuming our s-states and p-states are separately degenerate, would look something like figure 20 (a). The peak at 10 MeV. represents production of the $(1s)_{\Lambda}$ state. The peak at 1.0 MeV. represents the production of the $(1p)_{\Lambda}$ state. However if one considers the situation somewhat more carefully the results would look more like figure 20 (b). The strength to the (1s) state is now spread into 4 states while the (1p) state strength is almost completely washed out by the large number of states. It is clear from these simple considerations that it may be very difficult in point of fact to see the excited states "p-states" when experimentally one must fight both the π^- background associated with K-beams and the problems of good resolution, so necessary for meaningful interpretation of the data.

Furthermore, one is faced with absorptive effects associated with the finite size of the nucleus and the other reactions which could remove kaons from undergoing reaction (1). In our calculations, no account was taken of these absorptive effects, but estimates (Chapter 1) of those effects are something like a correction factor of 2 or 3 down from our calculated results. These estimates are not excessive or outrageous. They are related to the total K-N cross section (Kolbig, K.S., Margolis, B., 1968). When all these effects are put together it appears that the production of the lowest s-state will be less than 0.5 mb/st at 18° in the lab. For "p-states" of the lambda one is in much greater doubt about their observablity in these reactions, especially when one considers their low binding, background effects and finite resolution problems. But however difficult it may be to see these states, if they exist, if some selection rules operate then a careful experiment of this kind probably has as much chance seeing these states as any other. We eagerly await the experimental results.

APPENDIX 1

Scattering by a Many Body System

For completeness in this section, a summary of the formal theory of scattering of a particle by a general many body system is described, in order to show the relation of this scattering compared to the scattering from the separate constituents and to show the logical connection to the single scattering, impulse approximation. (Rodberg, S.L., and Thaler, R.M., 1967).

All approximations to the many body problem seek to reduce the problem to a series of two-body interactions. The multiple-scattering equations can be expressed in terms of two-body scattering amplitudes appropriate to the target.

Consider the scattering of a projectile by a complex target composed of N particles which may each interact with the projectile. If the target has a finite size, the incident projectile and the final outgoing particle will be free before and after the interaction respectively.

The initial and final states are described by the Hamiltonian

$$H_0 = K_0 + H_T \tag{1.1}$$

where K_0 is the kinetic energy operator for the projectile and H_T is the Hamiltonian for the target, including whatever interactions bind its constituents together. Let ϕ_λ be eigenstates of H_0. To distinguish the many body operators from two-body operators, upper and lower case symbols are used respectively. The projectile-target interaction is the sum of two-body interactions

$$V = \sum_{n=1}^{N} v_n \tag{1.2}$$

where v_n is the interaction between the projectile and particle n of the target. In inelastic processes, v_n may be an operator which creates and destroys particles. For example in the reaction $K^- + n \rightarrow \Lambda + \pi^-$, v_n annihilates the kaon and neutron and produces a lambda and pion in the final state.

The final outgoing state is given by the integral equation

$$\begin{aligned} \psi_i^{(+)} &= \phi_i + \frac{1}{E - H_0 + i\epsilon} V \psi_i^{(+)} \\ &= \phi_i + \frac{1}{E - H_0 + i\epsilon} \sum_{n=1}^{N} v_n \psi_i^{(+)} \end{aligned} \tag{1.3}$$

with ϕ_i the initial free particle state (Schiff, L., 1970). The transition amplitude for elastic or inelastic scattering is

$$T_{fi} = \langle \phi_f | \sum_{n=1}^{N} v_n | \psi_i^{(+)} \rangle \quad . \tag{1.4}$$

If the potenial V is sufficiently weak, T_{fi} may be expanded in powers of V. But a more general result, separates two-body effects from the multiple-scattering effects. It is possible to completely describe the scattering by a single particle and will generate a series showing a succession of scattering by different target particles.

Equations (1.3) and (1.4) can be rewritten as

$$\psi_i^{(+)} = \phi_i + \frac{1}{E - H_0 + i\epsilon} \sum_{n=1}^{N} t_n \psi_n \tag{1.5}$$

$$\psi_n = \phi_i + \frac{1}{E - H_0 + i\epsilon} \sum_{m \neq n}^{N} t_m \psi_m \tag{1.6}$$

$$t_n = v_n + v_n \frac{1}{E - H_0 + i\epsilon} t_n \tag{1.7}$$

and (1.8)

$$T_{fi} = \langle \phi_f | \sum_{n=1}^{N} t_n | \psi_n \rangle \quad .$$

This additional complexity is justified by the fact that these equations provide a description of the scattering process in terms of a multiple-scattering sequence. Substituting Eq. (1.6) and (1.5) we expand T_{fi} in powers of the transition operator t_n

$$T_{fi} = \langle \phi_f | \sum_{n=1}^{N} t_n + \sum_{n,m\neq n}^{N} t_n \frac{1}{E-H_0+i\epsilon} t_m \tag{1.9}$$
$$+ \sum_{\substack{n \\ m\neq n \\ \ell\neq m}} t_n \frac{1}{E-H_0+i\epsilon} t_m \frac{1}{E-H_0+i\epsilon} t_\ell + \cdots \quad |\phi_i\rangle$$

Each term in this series is a multiple-scattering sequence in which the projectile scatters successively from different particles in the medium. In the first term the projectile enters the target, scatters from particle n, and emerges. In the double scattering term the projectile scatters from m, propagates to particle n, where it scatters again and then emerges.

Single Scattering

If the target is sufficiently small, then only one scattering is likely to occur, then T_{fi} may be approximated by the first term in Eq. (1.9). It will be a valid assumption if the target thickness is small compared to the mean free path of the projectile. With this assumption

$$T_{fi} = \sum_{n=1}^{N} \langle \phi_f | t_n | \phi_i \rangle \tag{1.10}$$

This expression for the transition operator is still rather complicated, because it requires knowledge of t_n in the target, but it may be evaluated if the impulse approximation invoked. The impulse approximation basically replaces the two body transition operator t_n by the free two-body transition amplitude t_n^{free}, for the elementary process on one of the free particles in the target

$$T_{fi} = \sum_{n=1}^{N} \langle \phi_f | t_n^{\text{free}} | \phi_i \rangle \tag{1.11}$$
$$= \sum_{n=1}^{N} \langle f | t_n^{\text{free}} | i \rangle \, \mathcal{F}_{fi}(q)$$

where $\mathcal{F}_{fi}(q)$ is the Fourier Transform of the product of the initial target wave function and the final residual system's wave function. The last equation above is the high energy approximation, where one assumes that the t_n^{free} is not a strong function of the momentum of the struck particle. In the case under consideration, the struck neutron has a much smaller momentum than the incident kaon and hence this approximation would probably be rather good. If all the target particles are identical

(1.12) $$T_{fi} = N \langle f | t^{\text{free}} | i \rangle \mathcal{F}_{fi}(q)$$

The differential cross section in the center of momentum, is given by

$$\left(\frac{d\sigma}{d\Omega}\right) = \frac{1}{64\pi^2 S} \left|\frac{p_f}{p_i}\right| |T_{fi}|^2$$

(1.13) $$= N \cdot \frac{s}{S} \left|\frac{p_f}{p_i}\right| \left|\frac{k_i}{k_f}\right| |\mathcal{F}_{fi}(q)|^2 \left(\frac{d\sigma}{d\Omega}\right)_{\text{free}}$$

$$= N \cdot \rho(E) \cdot |\mathcal{F}_{fi}(q)|^2 \left(\frac{d\sigma}{d\Omega}\right)_{\text{free}}$$

with p_f, p_i are the final and incident momenta of the particles in the center of momentum of the target-projectile system, k_i, k_f are the initial and final momenta in the equivalent system for the elementary process under discussion and S, s are the total energy squared of the target-projectile and the nucleon-projectile systems respectively.

The assumption of replacing the two-body scattering amplitude t_n by the free K^-N amplitude implies that the structure of the target nucleus has no dynamical effect on the elementary process under consideration. The corrections to the impulse approximation involve the nuclear structure corrections and these are closely related to the multiple scattering corrections.

Furthermore the impulse approximation assumes that one knows the free T matrix off the energy shell. In practice one must extrapolates the off-shell value from the on-shell T matrix for similiar kinematics. The structure of the target system then only enters the impulse approximation in a kinematical way and higher order corrections in the multiple scattering theory may be calculated using the extrapolated off-shell T matrix.

APPENDIX 2

Why the factor $\sqrt{N}$ in T_{fi}.

In this appendix, we show how the factor of $\sqrt{N}$ in T_{fi} arises naturally, when one considers nuclear wave functions as Slater determinants, instead of the abstract fractional parentage coefficients used in Chapter 3.

To describe a nucleus with an independent particle model wave function, we start with a nuclear Hamiltonionian for N identical fermions:

(2.1) $$H_{Nucleus} = \sum_{i=1}^{N} H_{sp}(i)$$

with $$H_{sp}(i) = T(i) + V(r_i)$$

The single particle potential, $V(r)$ may be a Woods-Saxon, square well or harmonic oscillator potential. The nuclear wave function is then a pure Slater determinant

(2.2) $$\chi_N(1,2,\cdots,N) = \frac{1}{\sqrt{N!}} \begin{vmatrix} \phi_{\alpha_1}(1) & \phi_{\alpha_1}(2) & \cdots & \phi_{\alpha_1}(N) \\ \phi_{\alpha_2}(1) & \phi_{\alpha_2}(2) & \cdots & \phi_{\alpha_2}(N) \\ \vdots & \vdots & \ddots & \vdots \\ \phi_{\alpha_N}(1) & \phi_{\alpha_N}(2) & \cdots & \phi_{\alpha_N}(N) \end{vmatrix}$$

where the single particle wave functions $\phi_{\alpha_i}(j)$ are the solutions of the Schrödinger equation

(2.3) $$\{T_i + V(r_i)\}\phi_\alpha(r_i) = \epsilon_\alpha \phi_\alpha(r_i)$$

The normalization is

(2.4) $$\int |\phi_\alpha(r)|^2 d^3r = 1$$

and $$\int |\chi_N|^2 d^3r_1 d^3r_2 \cdots d^3r_N = 1$$

Consider the reaction $K^- + \text{nucleus} \rightarrow \text{nucleus}_\Lambda + \pi^-$. In order to extract the two-body matrix elements of reaction $K^- + n \rightarrow \Lambda + \pi^-$, we can write the Slater determinant in terms of the co-factors of one of the columns as

(2.5) $$\chi_N(1\cdots N) = \sum_{\alpha=\alpha_1}^{\alpha_N} \frac{\phi_\alpha(1)}{\sqrt{N}} \chi_{N-1}(2,3,\cdots,N)$$

where the expansion has been choosen so that

$$(2.6) \qquad \int |\chi_{N-1}(2,\cdots,N)|^2 d^3r_2 d^3r_3 \cdots d^3r_N = 1$$

Since all the particles are identical, it is only necessary to consider the interaction of the incident K-meson with particle 1. The initial state will be product of nuclear wave function and the relative motion between the center of mass of the nucleus and the incident K-meson

$$(2.7) \qquad \psi_i \sim \exp(i\,\underset{\sim}{k}_K(\underset{\sim}{r}_K - \underset{\sim}{r}_A))\,\chi_N$$

If we neglect multiple scattering effects and changes in the N-1 nucleus, the final state will be

$$(2.8) \qquad \psi_f \sim \exp(i\,\underset{\sim}{k}_\pi \cdot (\underset{\sim}{r}_\pi - \underset{\sim}{r}_{A\Lambda}))\,\chi_{N-1}\,\eta_\Lambda(r_\Lambda)$$

where $\eta_\Lambda(r)$ is the lambda wave function. The matrix element, neglecting center of mass motion, Clebsch-Gordan coefficients and other complications will be

$$T_{fi} \doteq \sum_\alpha \int \psi_f^* \, t \, \psi_i \, \delta^3(\underset{\sim}{r}_K - \underset{\sim}{r}_\pi)\,\delta^3(\underset{\sim}{r}_K - \underset{\sim}{r}_\Lambda)\,\delta^3(\underset{\sim}{r}_1 - \underset{\sim}{r}_\Lambda)\, d^3r_1 d^3r_2 \cdots d^3r_N\, d^3r_\Lambda \cdots d^3r_K$$

$$(2.9) \qquad \sim N \cdot t^{free} \cdot \int \exp(i\underset{\sim}{q}\cdot\underset{\sim}{r})\,\eta_\Lambda^*(\underset{\sim}{r})\,\frac{\phi_{\alpha_1}(r)}{\sqrt{N}}\,dr \cdot \int \chi_{N-1}^* \chi_{N-1}\, d\tau$$

$$\sim \sqrt{N} \cdot t^{free} \cdot \mathcal{F}_{fi}(\underset{\sim}{q})$$

$$|T_{fi}|^2 \doteq N\,|\mathcal{F}_{fi}(\underset{\sim}{q})|^2\,|t^{free}|^2$$

The factor $\sqrt{N}$ instead of N comes basically from the reaction being inelastic and the lack of anti-symmetry of the lambda-nuclear system. In elastic scattering the initial and final system would be anti-symmetric with respect to N particles and one would have a double sum over initial and final states resulting in a factor of N times the free transition amplitude.

Figure Captions

Figure 1: Diagramatic Interpretation of the K^--Nucleus Interaction.

Figure 2: The coefficients of the Legendre polynomial expansion Eq. (3) versus the incident K^- lab. momentum. Each of the curves is the result of a 9th order polynomial fit in momentum, to the coefficients obtained by averaging the K^--proton and K^--neutron results. (Adapted from Bonazzola, G.C., et al, 1970)

Figure 3: The experimental differential cross section for $K^- + n \rightarrow \Lambda + \pi^-$ at incident lab. momentum 777 MeV/c. measured in the center of mass.

Figure 4: This diagram illustrates the position of the nucleon relative to the (A-1) nuclear system and the overall center of mass. The notation is the same as is used in the text.

Figure 5: A plot of $u(r) = r R(r)$, where $R(r)$ is the radial wave function of the bound lambda in $^4He_\Lambda$. The peak in the wave function is reproduced by an appropriate Gaussian fit to $R(r)$ when a oscillator parameter of $a_\Lambda = 1.90$ fm. is used. The depth of the well, which reproduced the known binding energy of 2.25 MeV/c., was 29.34 MeV.

Figure 6: Differential cross section for the production of $^4He_\Lambda$ at incident kaon momentum of 800 MeV/c.

Figure 7: Differential cross sections for $^4He_\Lambda$ production at incident kaon momenta (a) 500 MeV/c., (b) 600 MeV/c., and (c) 700 MeV/c.

Figure 8: Differential cross sections for the production of $^{12}C_\Lambda$ at 500 MeV/c. Curve (a) corresponds to a sum over the states of the

configuration $(1p)^{-1}_n(1s)_\Lambda$. Curve (b) corresponds to a sum over the states of the configuration $(1p)^{-1}_n(1p)_\Lambda$.

Figure 9: Differential cross sections for the production of $^{12}C_\Lambda$ at 600 MeV/c.

Figure 10: Differential cross sections for the production of $^{12}C_\Lambda$ at 700 MeV/c.

Figure 11: Differential cross sections for the production of $^{12}C_\Lambda$ at 800 MeV/c.

Figure 12: A plot of $u(r) = r R(r)$, where $R(r)$ is the radial wave function of the bound lambda in $^{12}C_\Lambda$ in p-state. The peak in the wave function is reproduced by a 3-dimensional harmonic oscillator wave function with an oscillator parameter $a_\Lambda = 1.76$ fm. The depth of the well, which reproduced the assumed binding of 0.5 MeV. was 37.06 MeV.

Figure 13: A plot of $u(r) = r R(r)$, where $R(r)$ is the radial wave function of the bound lambda in $^{16}O_\Lambda$ in a p-state. The peak in the wave function is reproduced by a 3-dimensional harmonic oscillator wave function with an oscillator parameter $a_\Lambda = 1.91$ fm. The depth of the well, which reproduced the assumed binding of 1.0 MeV. was 30.61 MeV.

Figure 14: Differential cross sections for the production of $^{16}O_\Lambda$ at 500 MeV/c.

Figure 15: Differential cross sections for the production of $^{16}O_\Lambda$ at 600 MeV/c.

Figure 16: Differential cross sections for the production of $^{16}O_\Lambda$ at 700 MeV/c.

Figure 17: Differential cross sections for the production of $^{16}O_\Lambda$ at 800 MeV/c.

Figures 18 and 19: The momentum transfer $|\vec{q}|$ as a function of the cosine of the scattering angle $\Theta_{c.m.}$ at incident kaon momenta 500, 600, 700 and 800 MeV/c. for $^4He_\Lambda$ and $^{16}O_\Lambda$ respectively. The dashed line corresponds to the momentum transfer resulting from a stopped K^--meson.

Figure 20: In this figure we try to interpret our results experimentially for $^{16}O_\Lambda$. (a) corresponds to the ideal case in which there is no background, the $(1p)_n^{-1}(1s)_\Lambda$ states are degenerate and similarly the $(1p)_n^{-1}(1p)_\Lambda$ states. The missing mass corresponds to the energy of any bound states that exist. The $(1p)_n^{-1}(1s)_\Lambda$ state has a binding of 10.0 MeV; and the $(1p)_n^{-1}(1p)_\Lambda$ state a binding of 1.0 MeV. In (b) we have tried to put some real physics into the picture. The $(1p)^{-1}(1s)_\Lambda$ states are split by roughly 6 MeV. and further by spin-spin interactions. The p-states are almost washed out by energy splitting and background.

REFERENCES

Ajzenberg-Selove, F., Nuclear Physics A152, 1, 1970.

Armenteros, R., et al, Nuclear Physics B8, 183, 1968.

Bonazzola, G.C., et al, CERN Internal Document, PH III 70/39.

Dalitz, R.H., Proc. 1962 Ann. Int. Conf. High Energy Physics, CERN, 1962.

Dalitz, R.H., Proceedings of International Conference on Hypernuclear Physics, High Energy Physics Division, Argonne National Lab. Argonne, Illinois, 1969.

Davis, D.H., and Sacton, J., Hypernuclear Physics in "High Energy Physics", Edited by E.H.S. Burhop, Vol.II, 1967, Academic Press, N.Y.

Elliott, J.P., and Lane, A.M., Encyclopaëdia of Physics, Vol. XXXIX, 1957.

Gal, A., Soper, J.M., and Dalitz, R.H., Annals of Physics 63, 53, 1971.

Goldberger, M.L., and Watson, K.M., Collision Theory, John Wiley and Sons, New York, 1964.

Iwao, S., Progress of Theoretical Physics, 46, 1407, 1971.

Kallen, G., Elementary Particle Physics, 1964, Addison-Wesley, London.

Kolbig, K.S., and Margolis, B., Nuclear Physics B6, 85, 1968.

Lock, L.O., and Measday, D.F., Intermediate Energy Nuclear Physics, 1970, Methuen and Co., London.

Martin, A.D., and Spearman, T.D., Elementary Particle Physics, 1970, North-Holland Publishing, Amsterdam.

McCarthy, I.E., Introduction to Nuclear Theory, 1968, J. Wiley and Sons, New York.

Middleton, E., M. Sc. Thesis, University of Liverpool, 1971.

Rodberg, S.L., and Thaler, R.M., Introduction to the Quantum Theory of Scattering, 1967, Academic Press.

Schiff, L., Quantum Mechanics - 2nd Edition, McGraw-Hill, 1970.

Shakin, C.M., Wihmare, Y.R., Hull, M.H., Physical Review 161, 1001, 1967

Tanner, N., Private Communication, 1971.

TABLE I

PARTICLE	MASS (MeV)	PARTICLE		MASS (MeV)
π	139.578	K		493.82
Λ	1115.60	n		939.55
^4He	3727.32	$^4He_\Lambda$; $(1s)_n^{-1}(1s)_\Lambda$		3910.44
^{12}C	11174.67	$^{12}C_\Lambda$	$(1p)_n^{-1}(1s)_\Lambda$	11357.44
			$(1p)_n^{-1}(1p)_\Lambda$	11366.44
^{16}O	14894.82	$^{16}O_\Lambda$	$(1p)_n^{-1}(1s)_\Lambda$	15073.53
			$(1p)_n^{-1}(1p)_\Lambda$	15082.53

	^4He	^{12}C	^{16}O
a_n	1.38 fm.	1.56 fm.	1.56 fm.
$a_\Lambda^{(1s)}$	1.90 fm.	1.74 fm.	1.90 fm.
$a_\Lambda^{(1p)}$		1.74 fm.	1.90 fm.

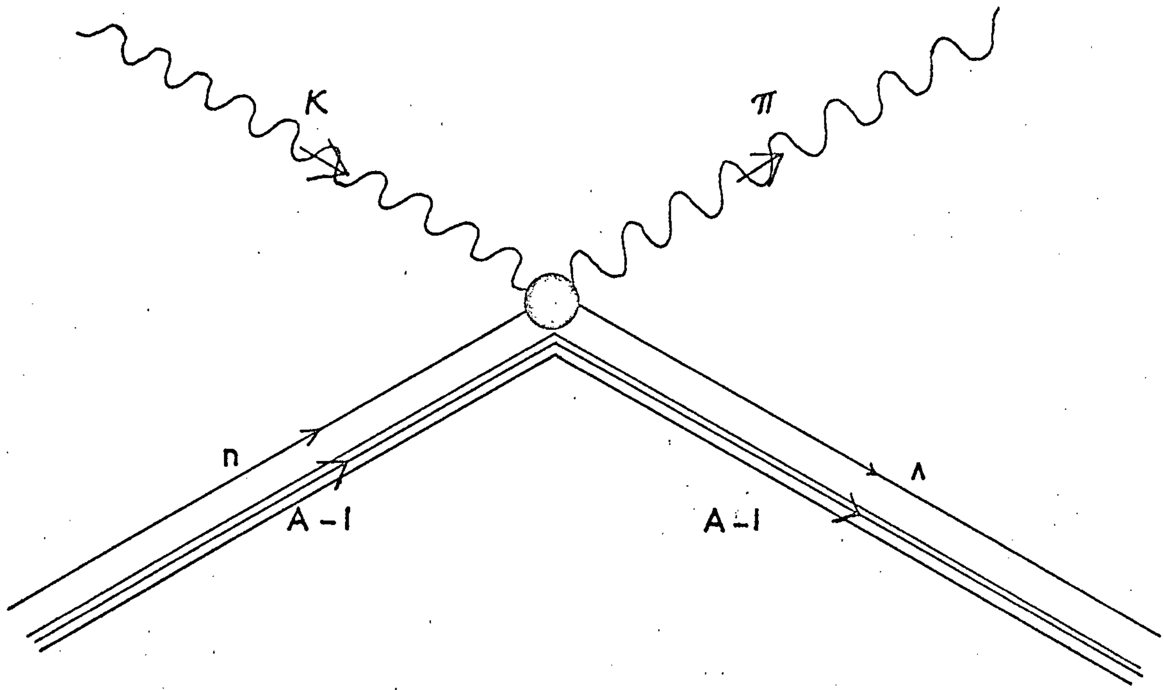

FIG. I

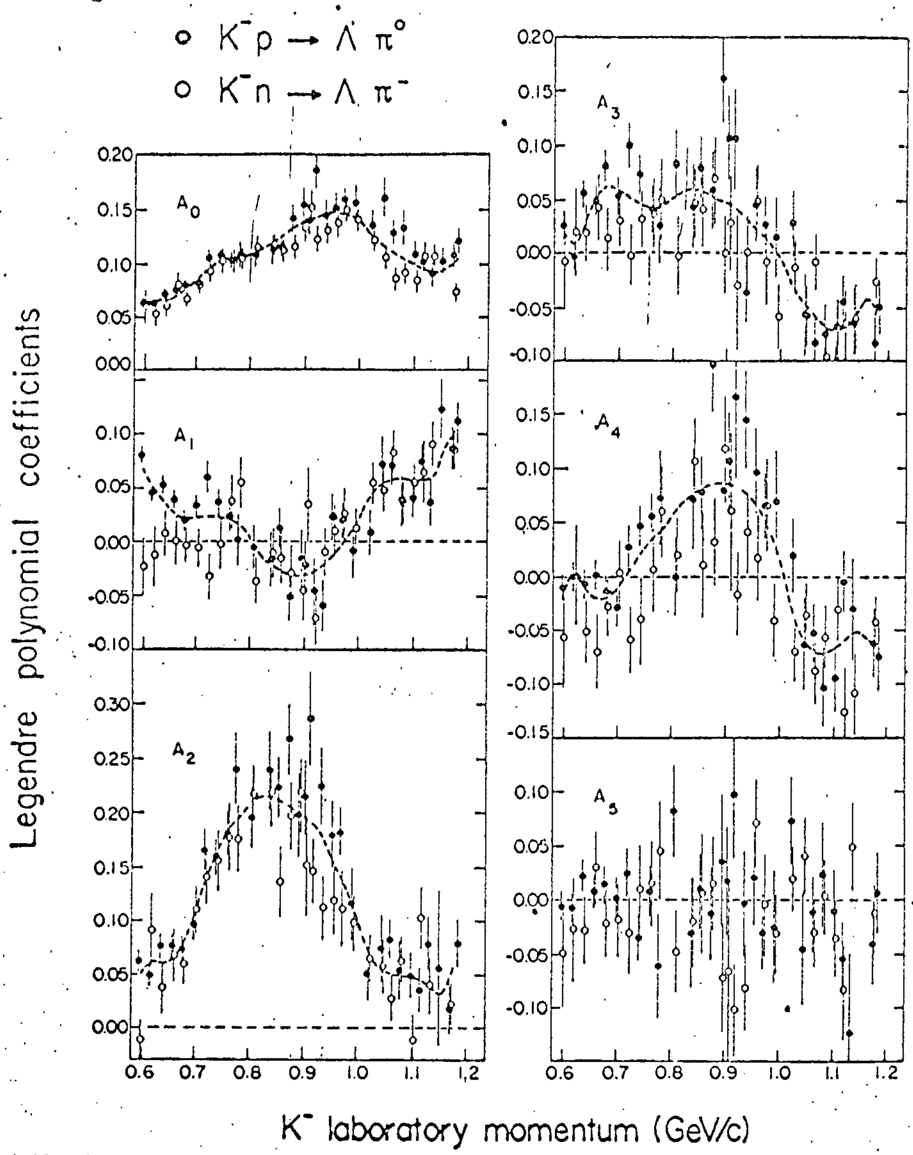

K⁻p → Λ π⁰
K⁻n → Λ π⁻
A0
A1
A2
A3
A4
A5
Legendre polynomial coefficients
K⁻ laboratory momentum (GeV/c)

FIG. 2

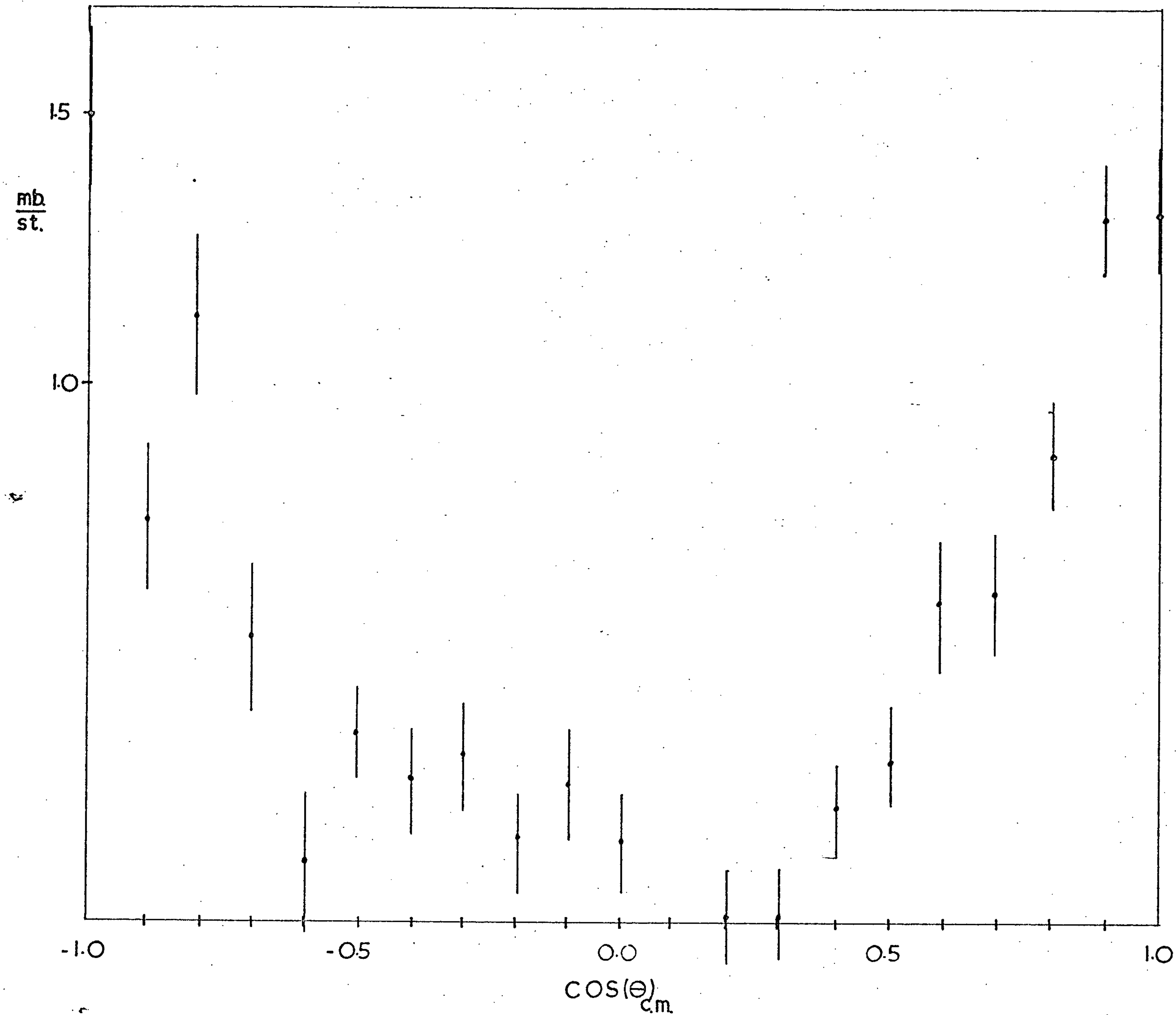

FIG. 3

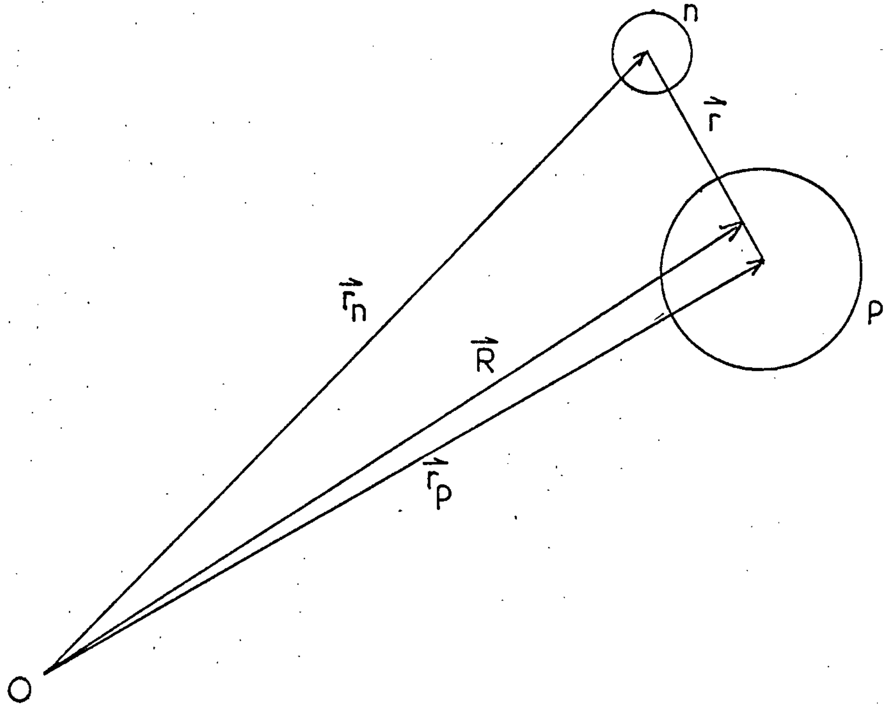

FIG. 4

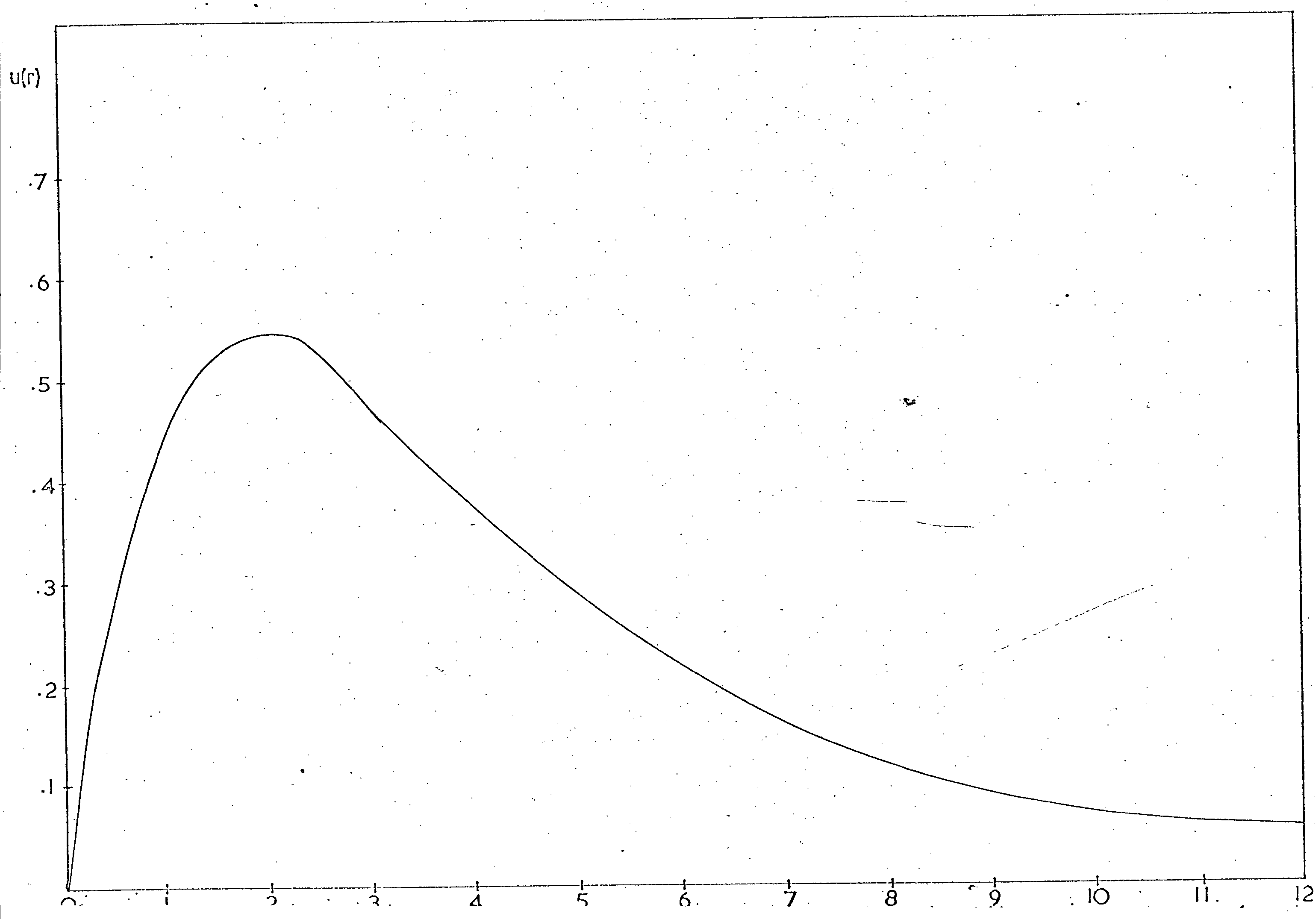

FIG. 5

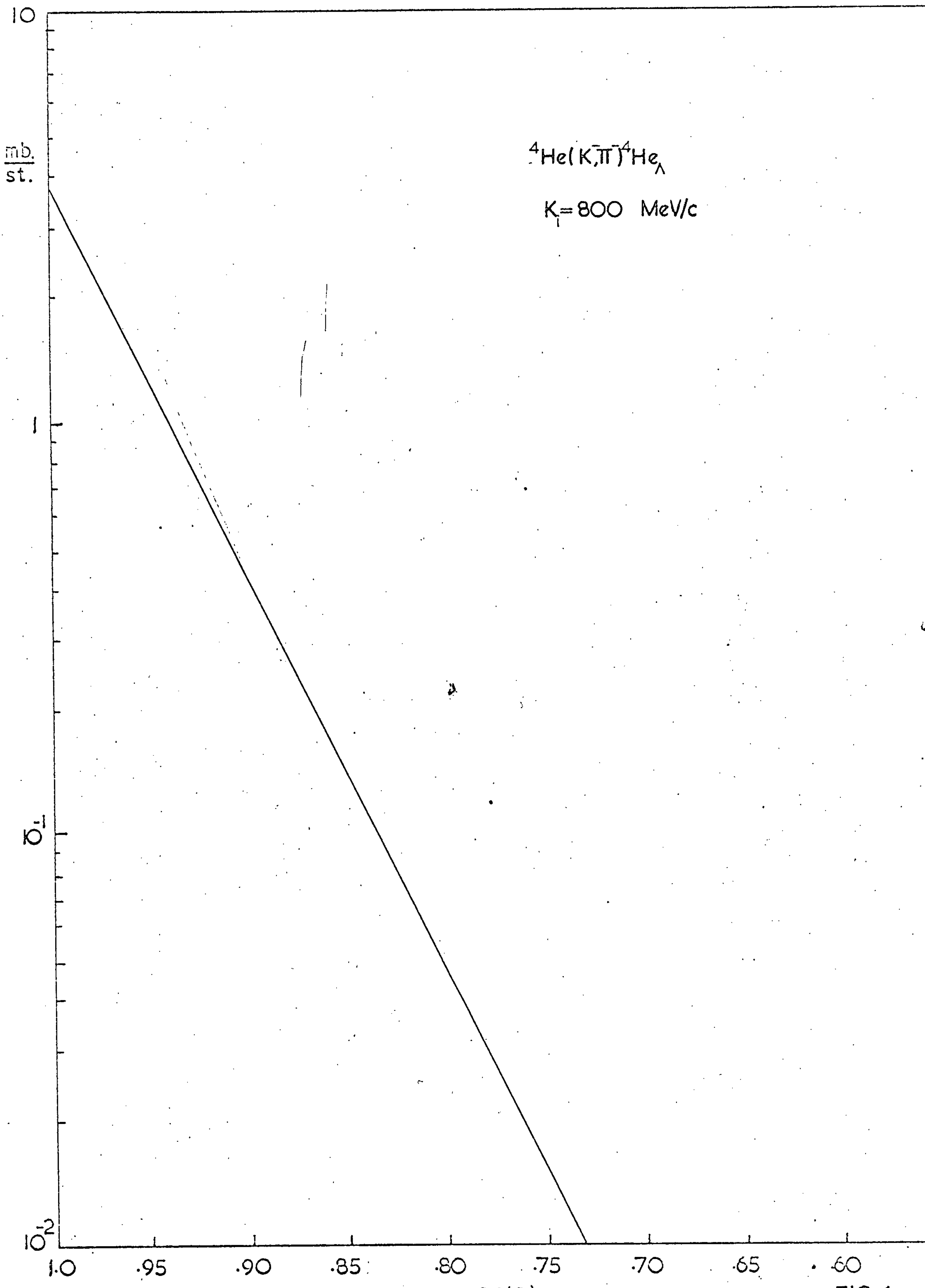

10
mb.
st.
1
10⁻¹
10⁻²
⁴He(K⁻,π⁻)⁴He$_\Lambda$
K$_i$= 800 MeV/c
1.0
.95
.90
.85
.80
.75
.70
.65
.60
COS(Θ)

FIG. 6

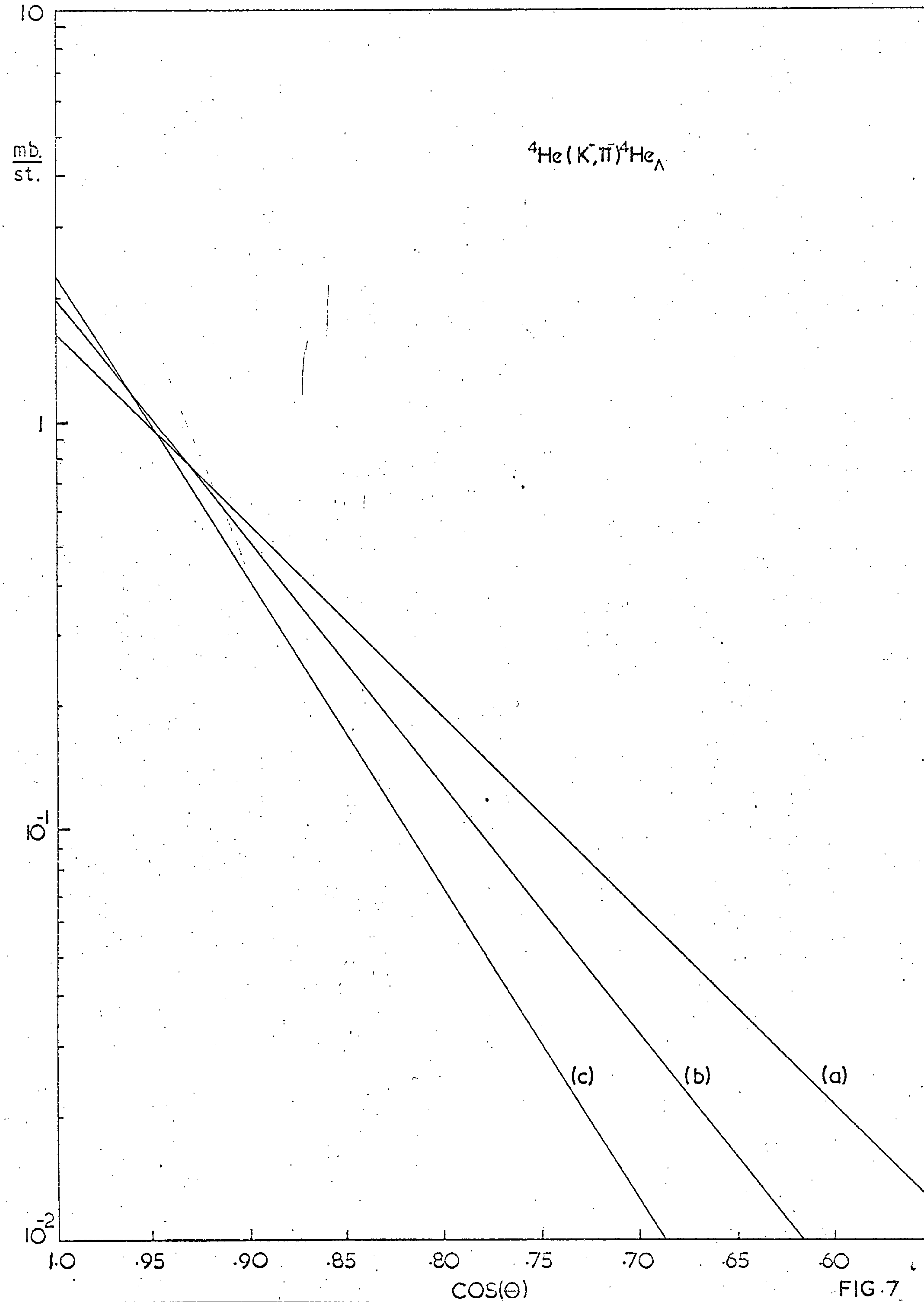

10
1
10^{-1}
10^{-2}
mb./st.
$^4He(K^-,\pi^-)^4He_\Lambda$
(c)
(b)
(a)
1.0
·95
·90
·85
·80
·75
·70
·65
·60
COS(Θ)

FIG·7

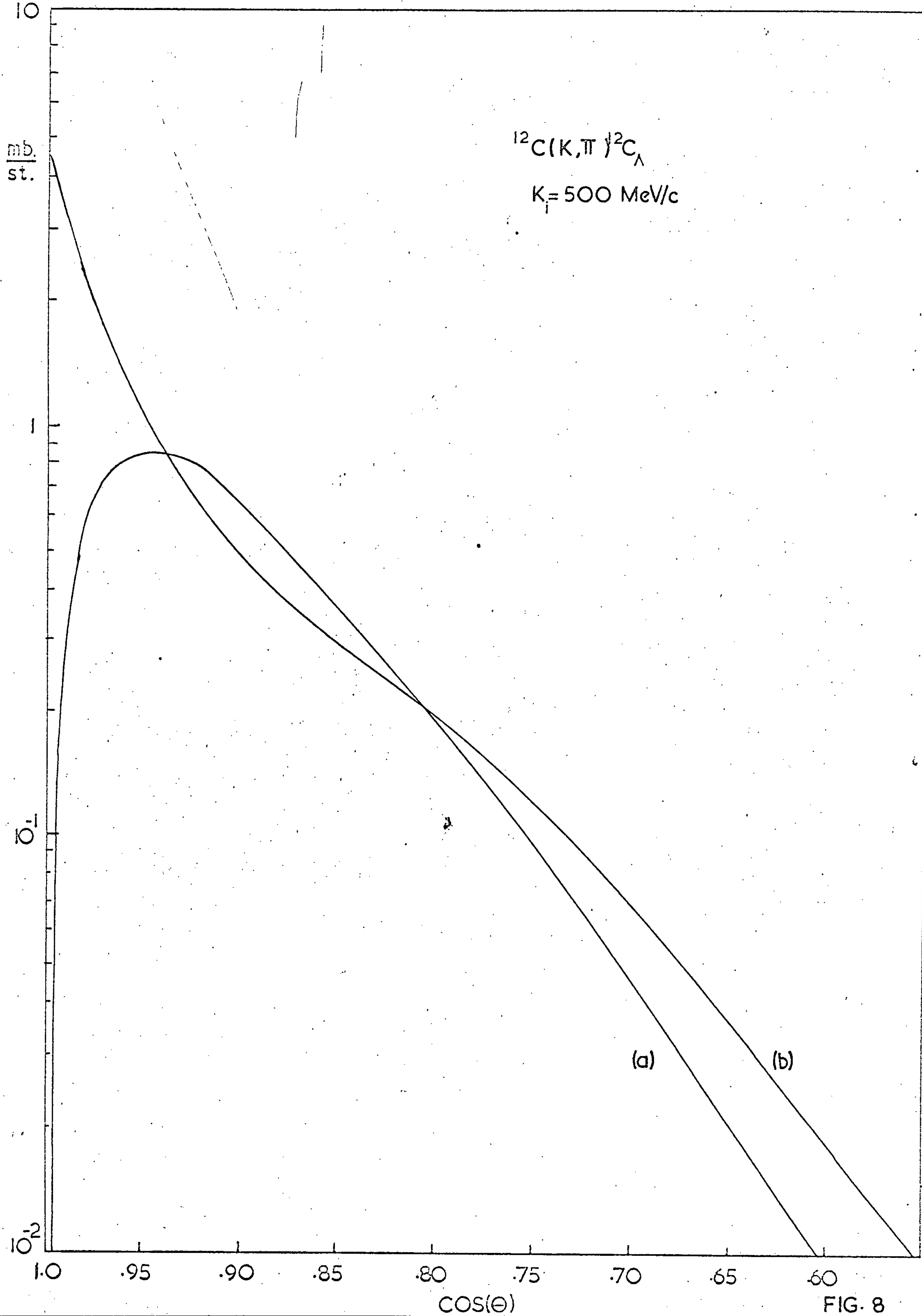

10
1
10^{-1}
10^{-2}
mb. / st.
$^{12}C(K,\pi)^{12}C_\Lambda$
K_i = 500 MeV/c
(a)
(b)
1.0
·95
·90
·85
·80
·75
·70
·65
·60
COS(Θ)

FIG. 8

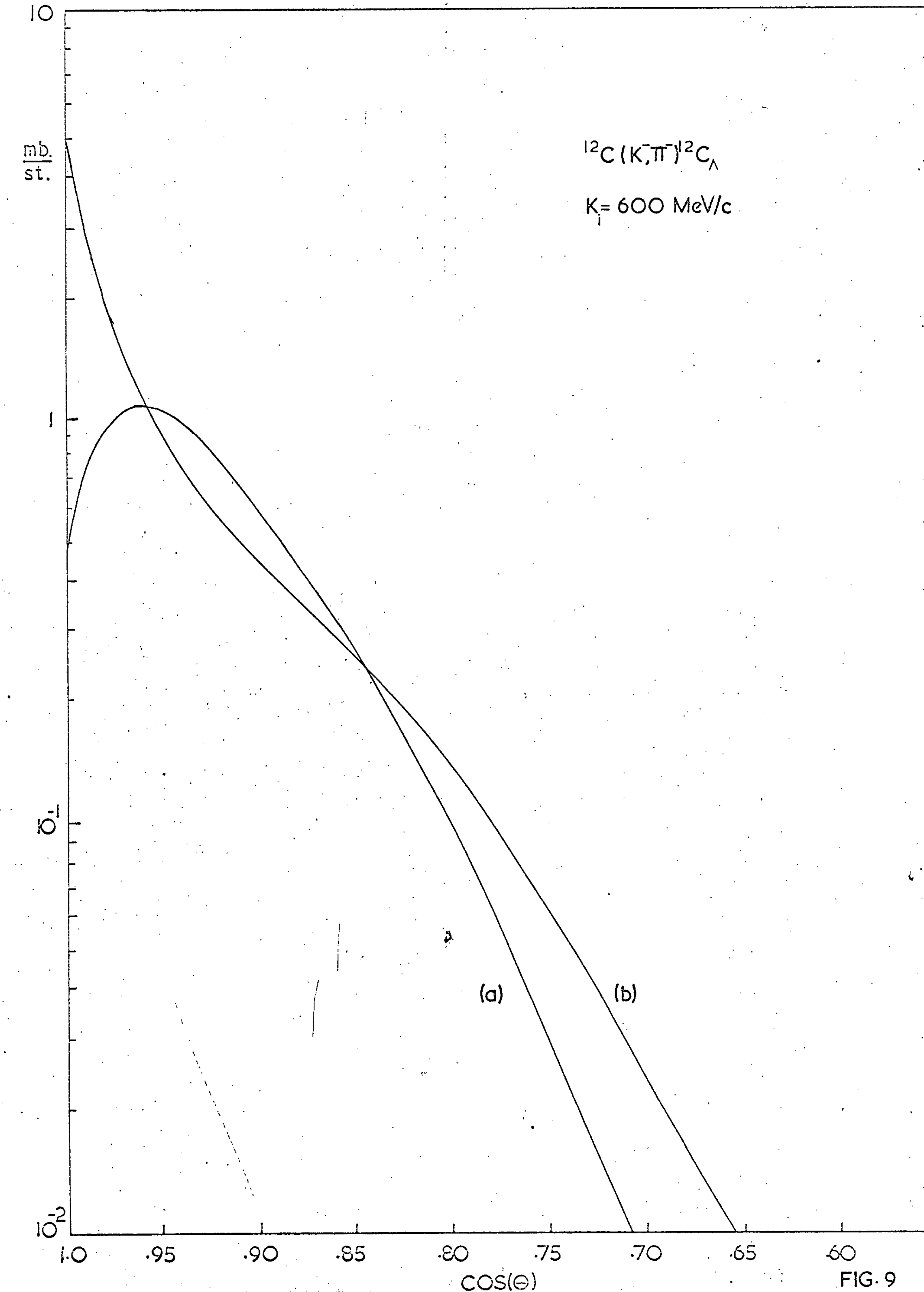
10
mb.
st.
$^{12}C(K^-,\pi^-)^{12}C_\Lambda$
K_i = 600 MeV/c
1
10^{-1}
(a)
(b)
10^{-2}
1.0
.95
.90
.85
.80
.75
.70
.65
.60
COS(Θ)

FIG. 9

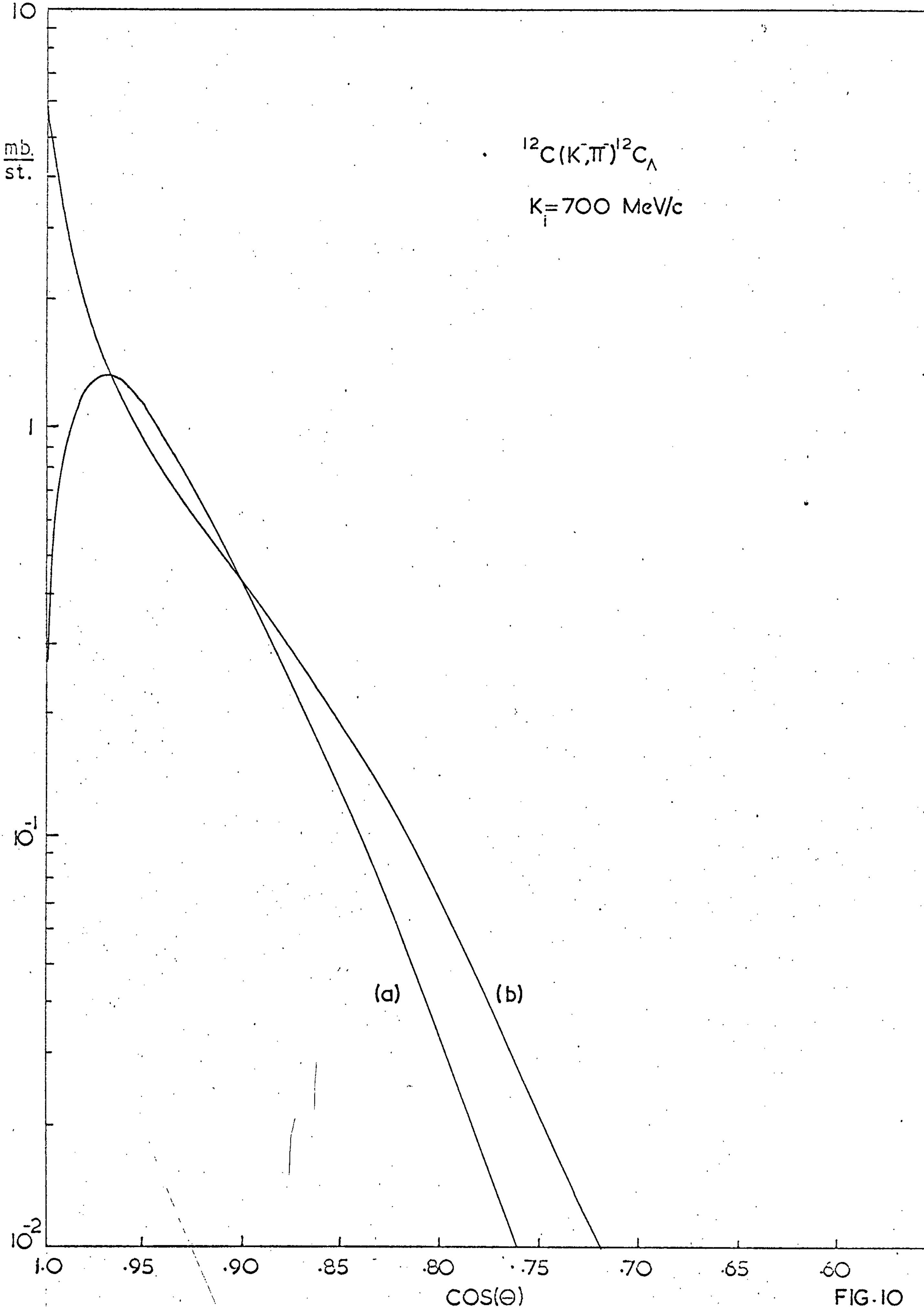
10
mb.
st.
$^{12}C(K^-,\pi^-)^{12}C_\Lambda$
$K_i = 700$ MeV/c
1
10^{-1}
(a)
(b)
10^{-2}
1.0
.95
.90
.85
.80
.75
.70
.65
.60
COS(Θ)
FIG. 10

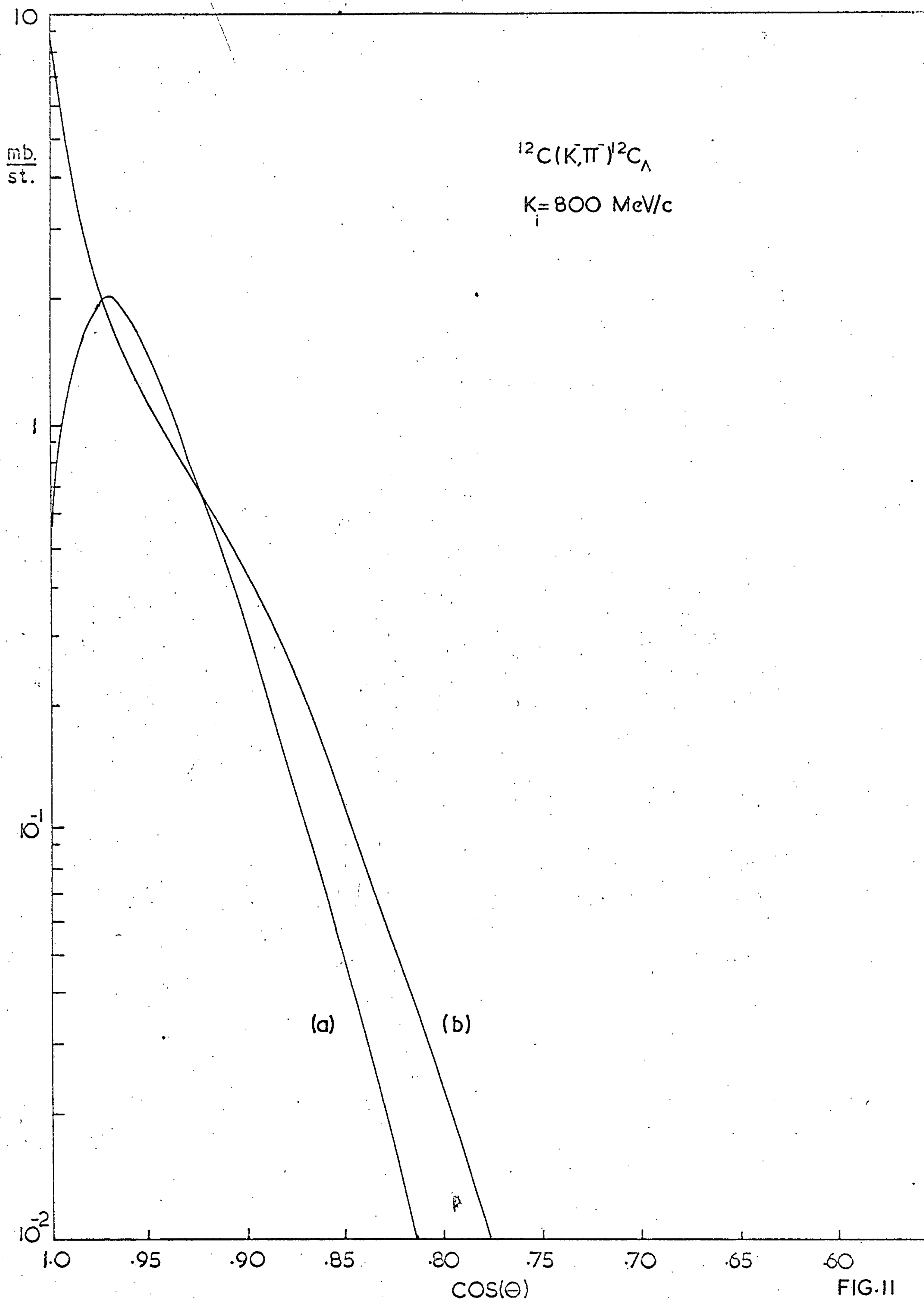

10
mb.
st.
1
10^{-1}
10^{-2}
$^{12}C(K^-,\pi^-)^{12}C_\Lambda$
$K_i = 800$ MeV/c
(a)
(b)
1.0
.95
.90
.85
.80
.75
.70
.65
.60
COS(Θ)

FIG.11

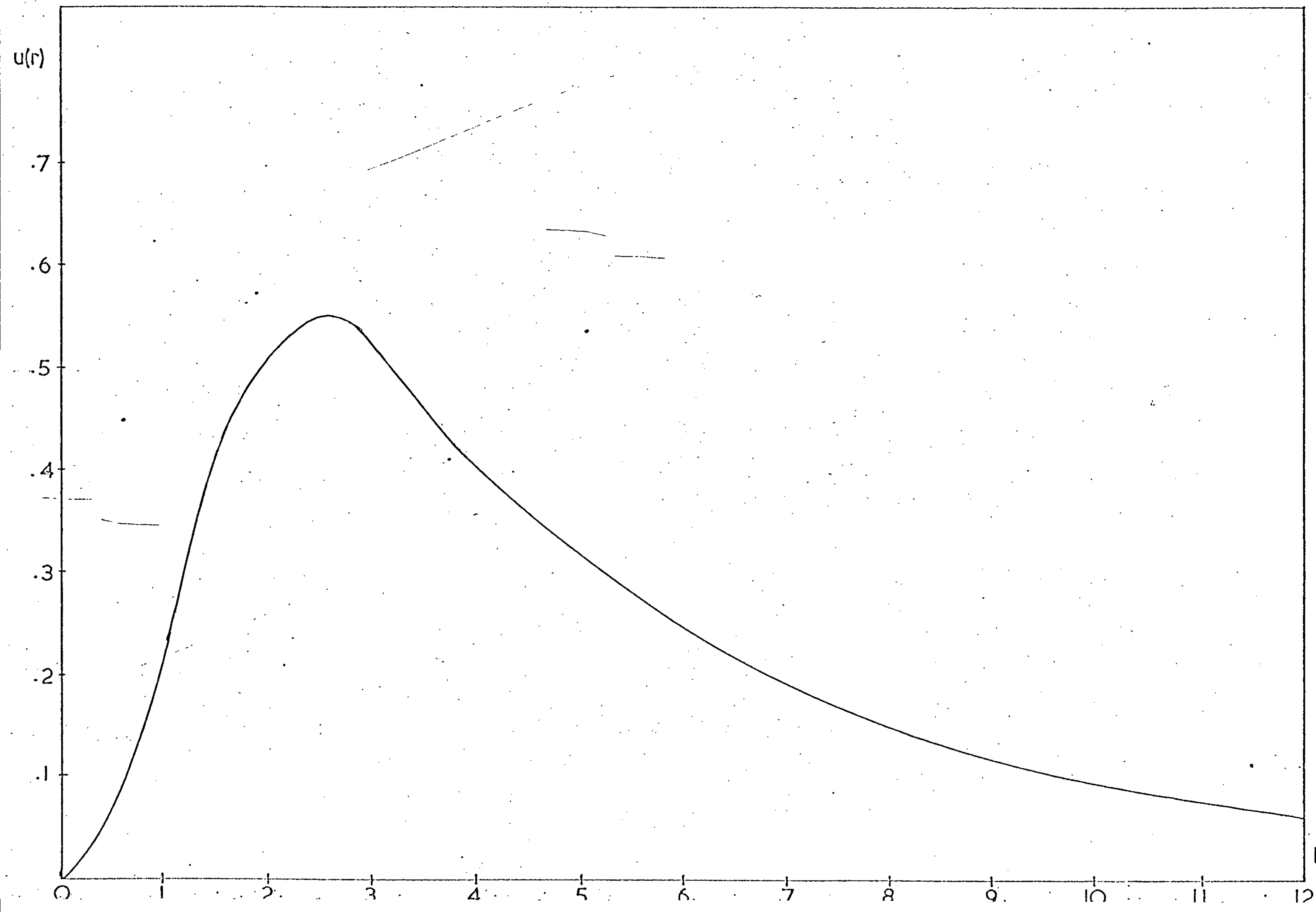

FIG. 12

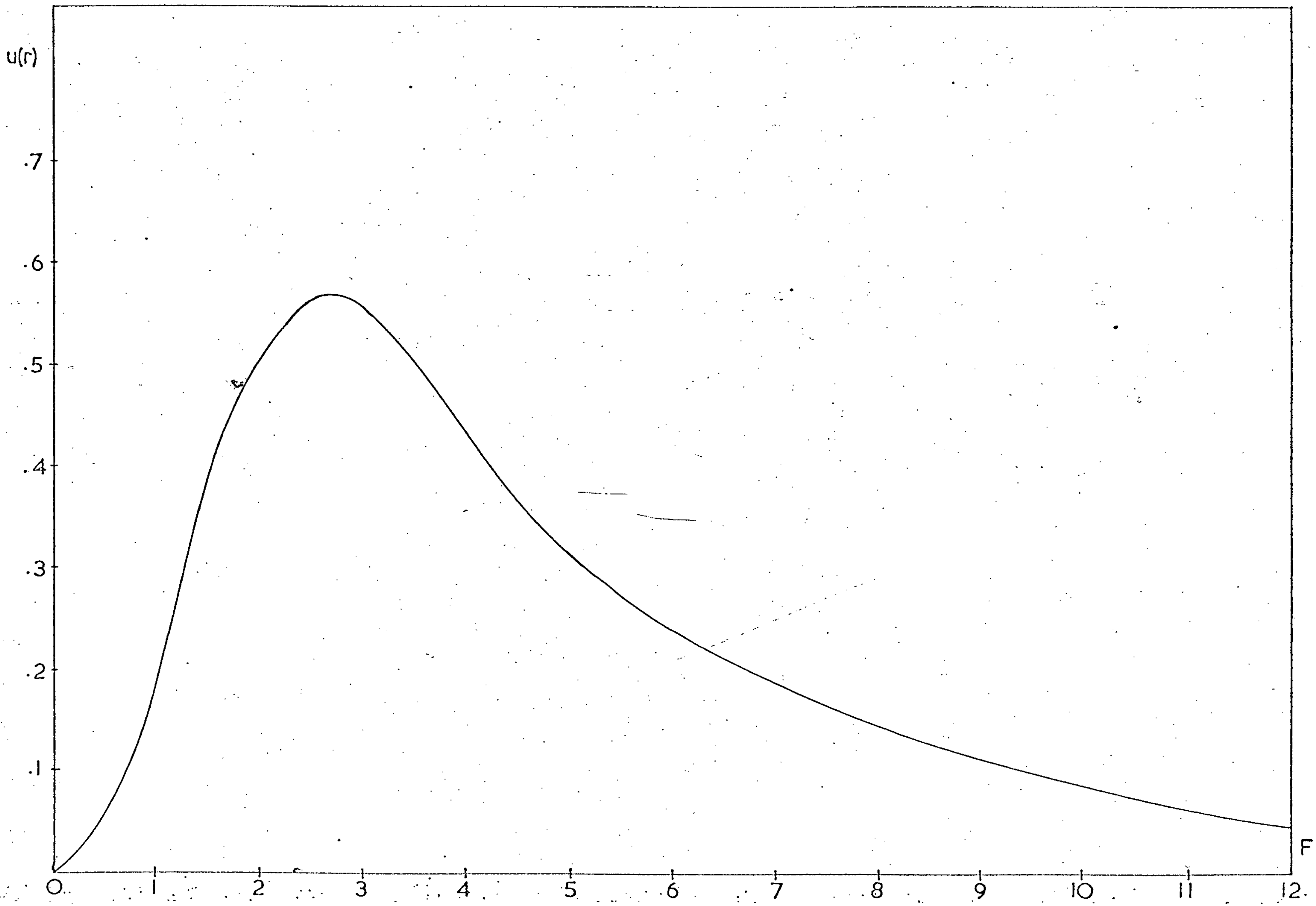

FIG. 13

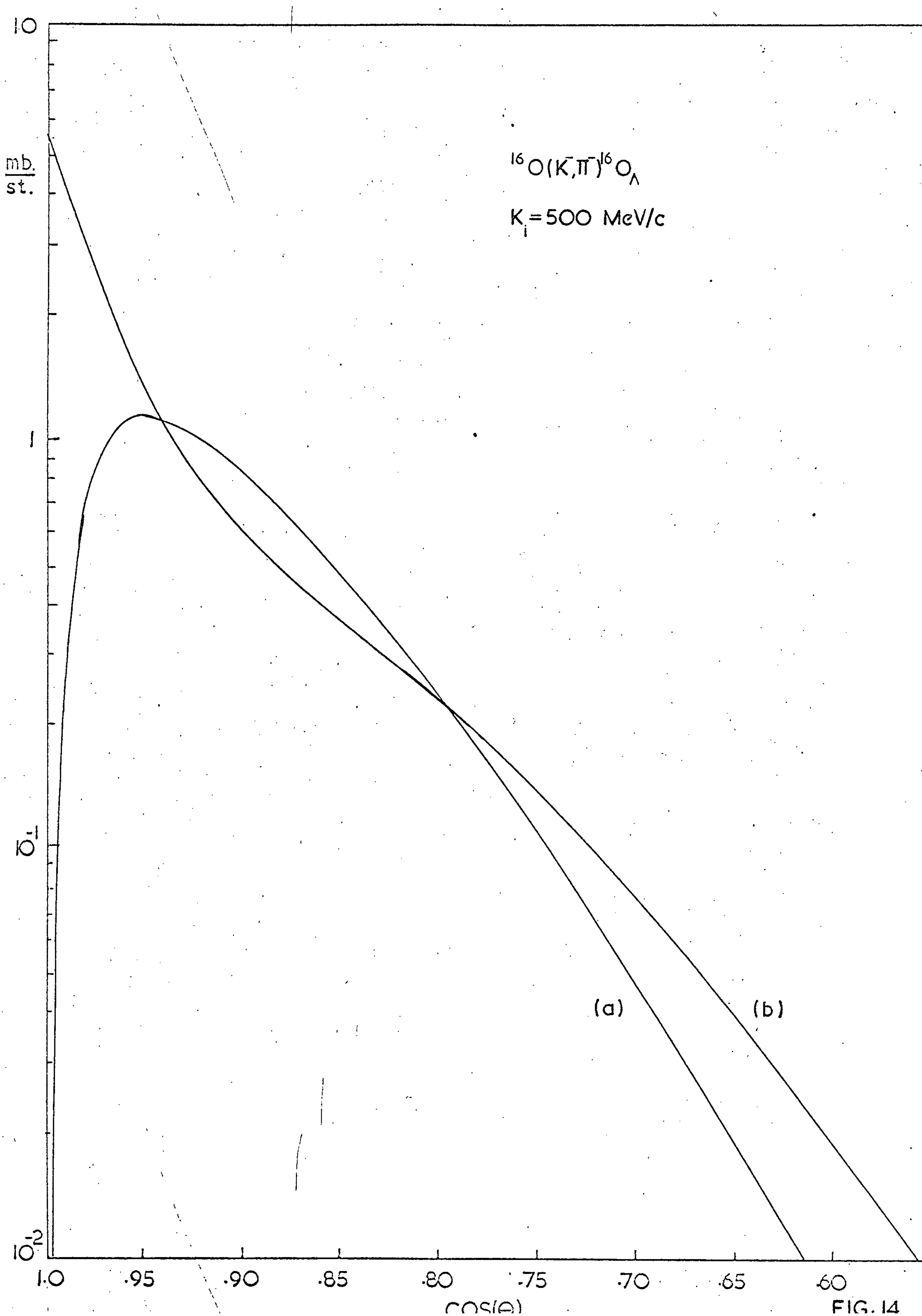

10
mb.
st.
$^{16}O(K^-,\pi^-)^{16}O_\Lambda$
$K_i = 500$ MeV/c
1
10^{-1}
10^{-2}
(a)
(b)
1.0
.95
.90
.85
.80
.75
.70
.65
.60
COS(Θ)

FIG. 14

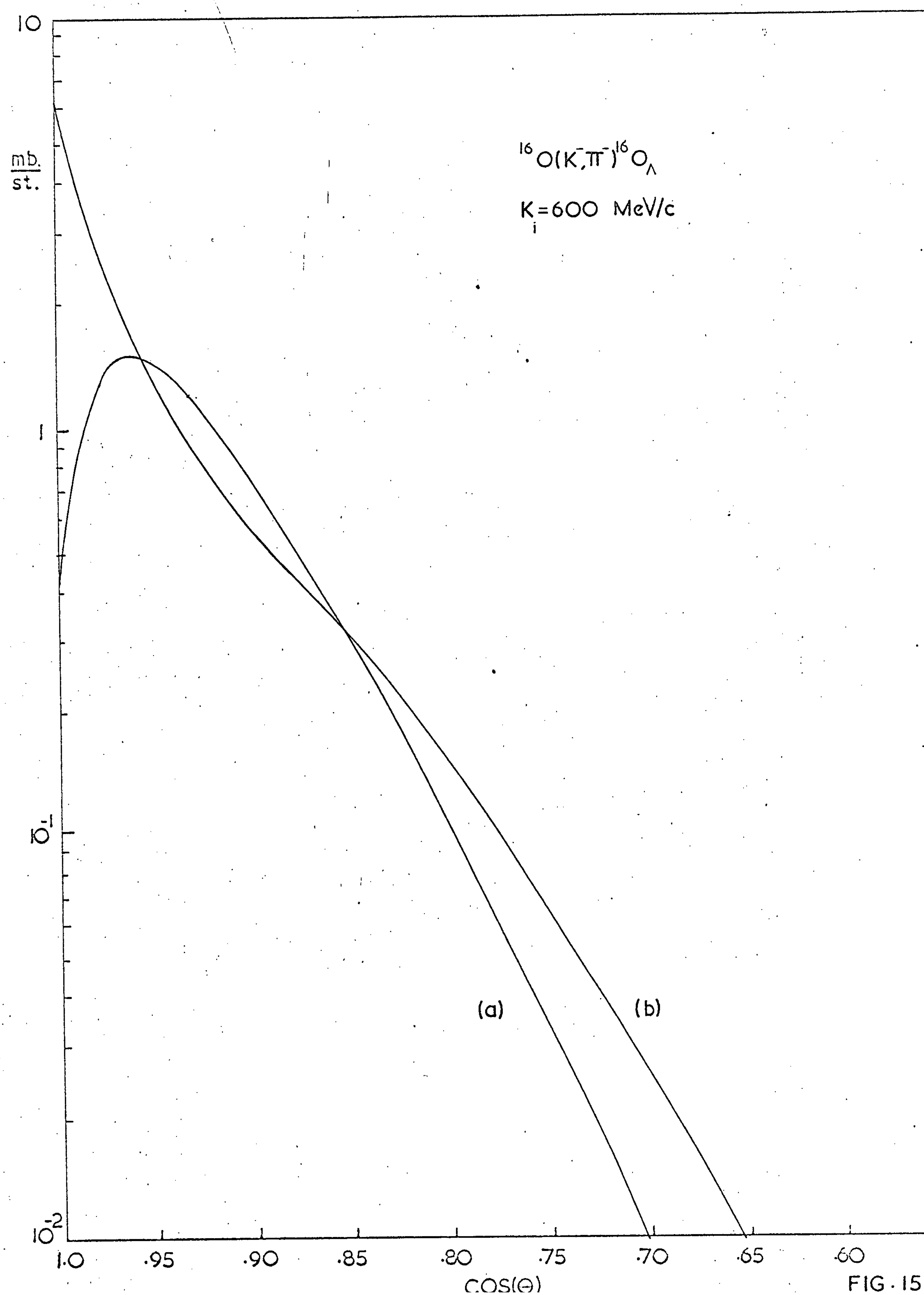

$^{16}O(K^-,\pi^-)^{16}O_\Lambda$
$K_i=600$ MeV/c
$\frac{mb.}{st.}$
10
1
10^{-1}
10^{-2}
(a)
(b)
1.0
.95
.90
.85
.80
.75
.70
.65
.60
COS(Θ)

FIG. 15

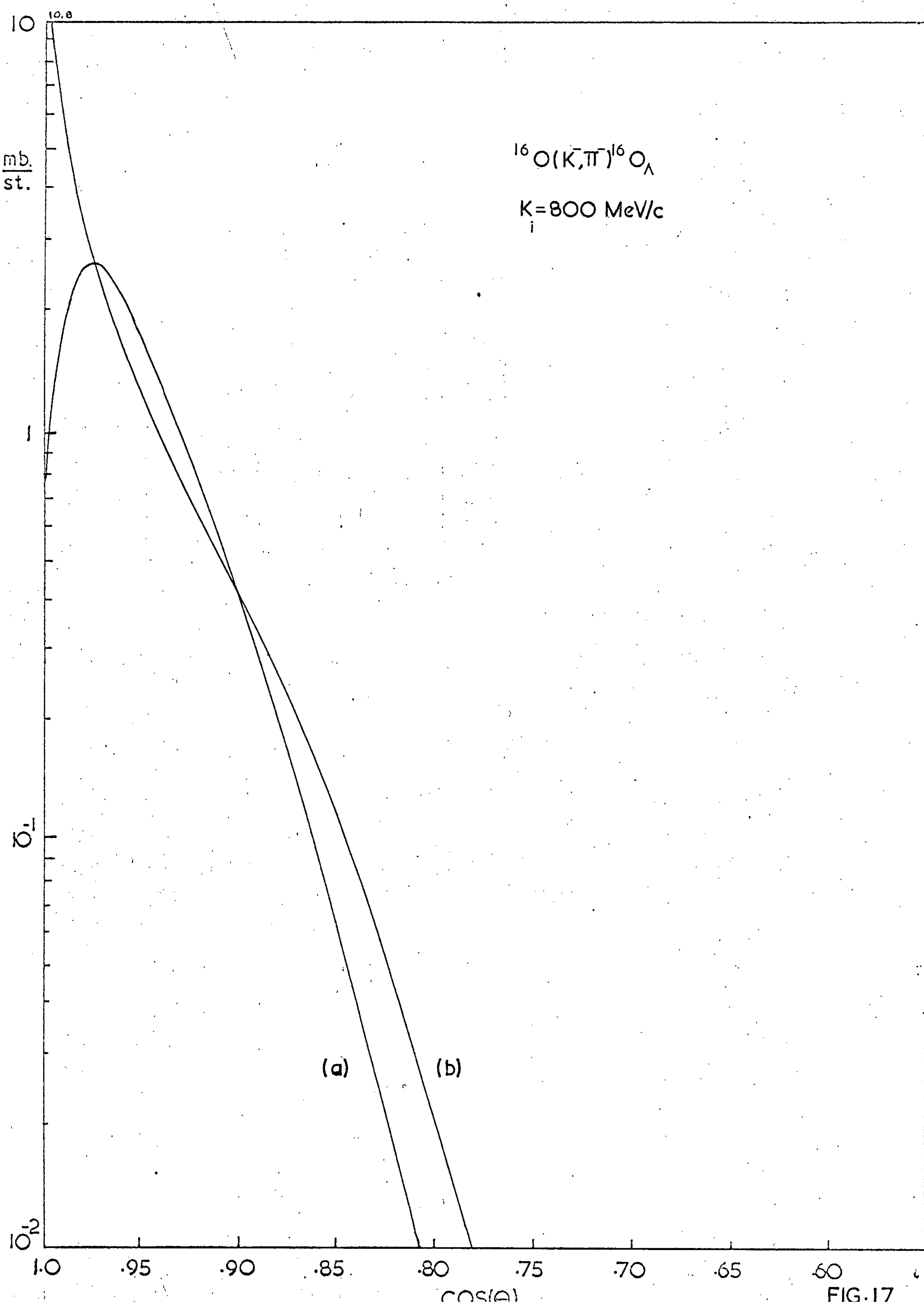

10.8
10
1
10^{-1}
10^{-2}
mb./st.
$^{16}O(K^-,\pi^-)^{16}O_\Lambda$
K_i=800 MeV/c
(a)
(b)
1.0
.95
.90
.85
.80
.75
.70
.65
.60
COS(Θ)

FIG.17

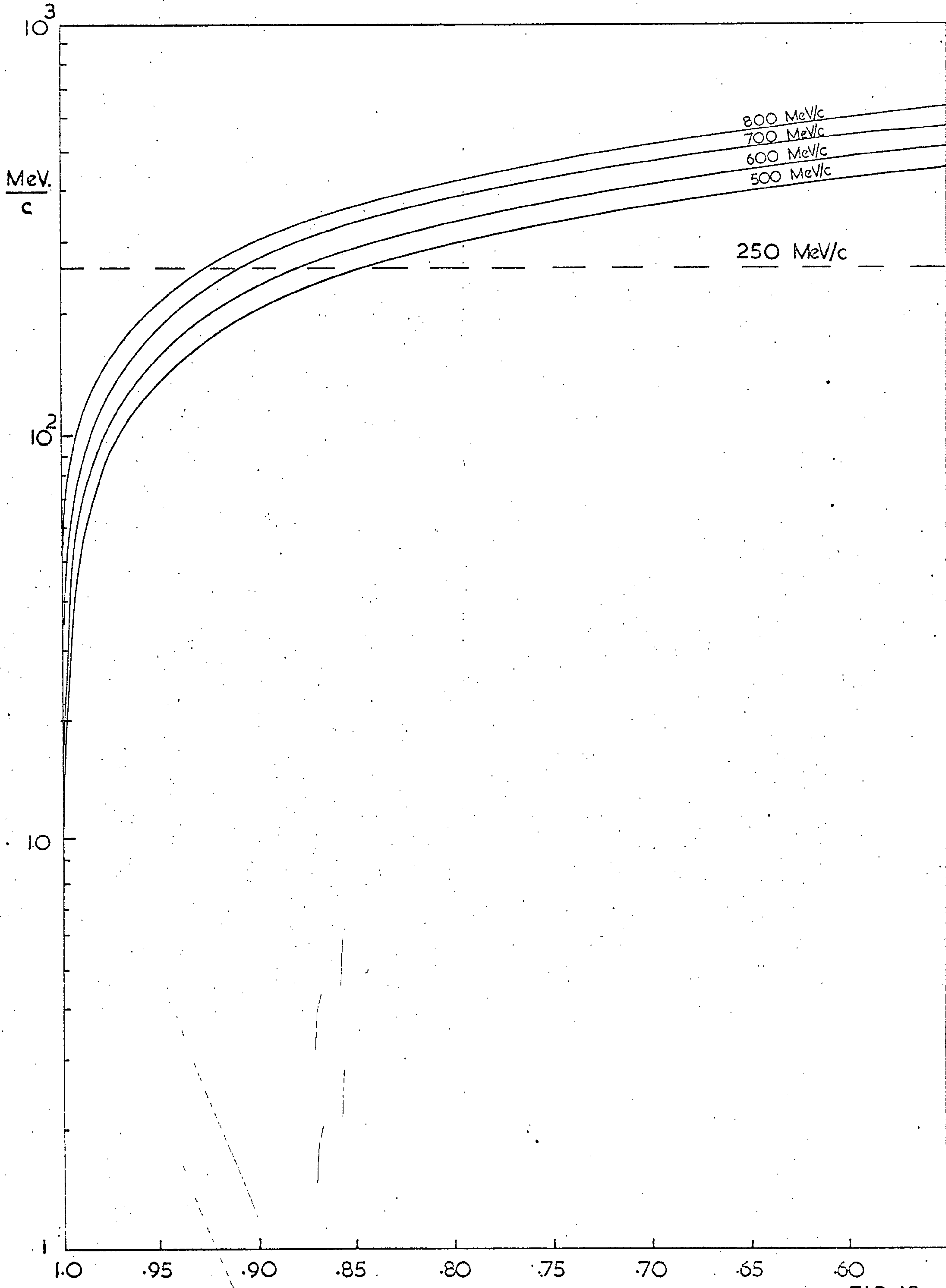

10^3
10^2
10
1
MeV. / c
800 MeV/c
700 MeV/c
600 MeV/c
500 MeV/c
250 MeV/c
1.0
.95
.90
.85
.80
.75
.70
.65
.60
COS(Θ)

FIG. 18

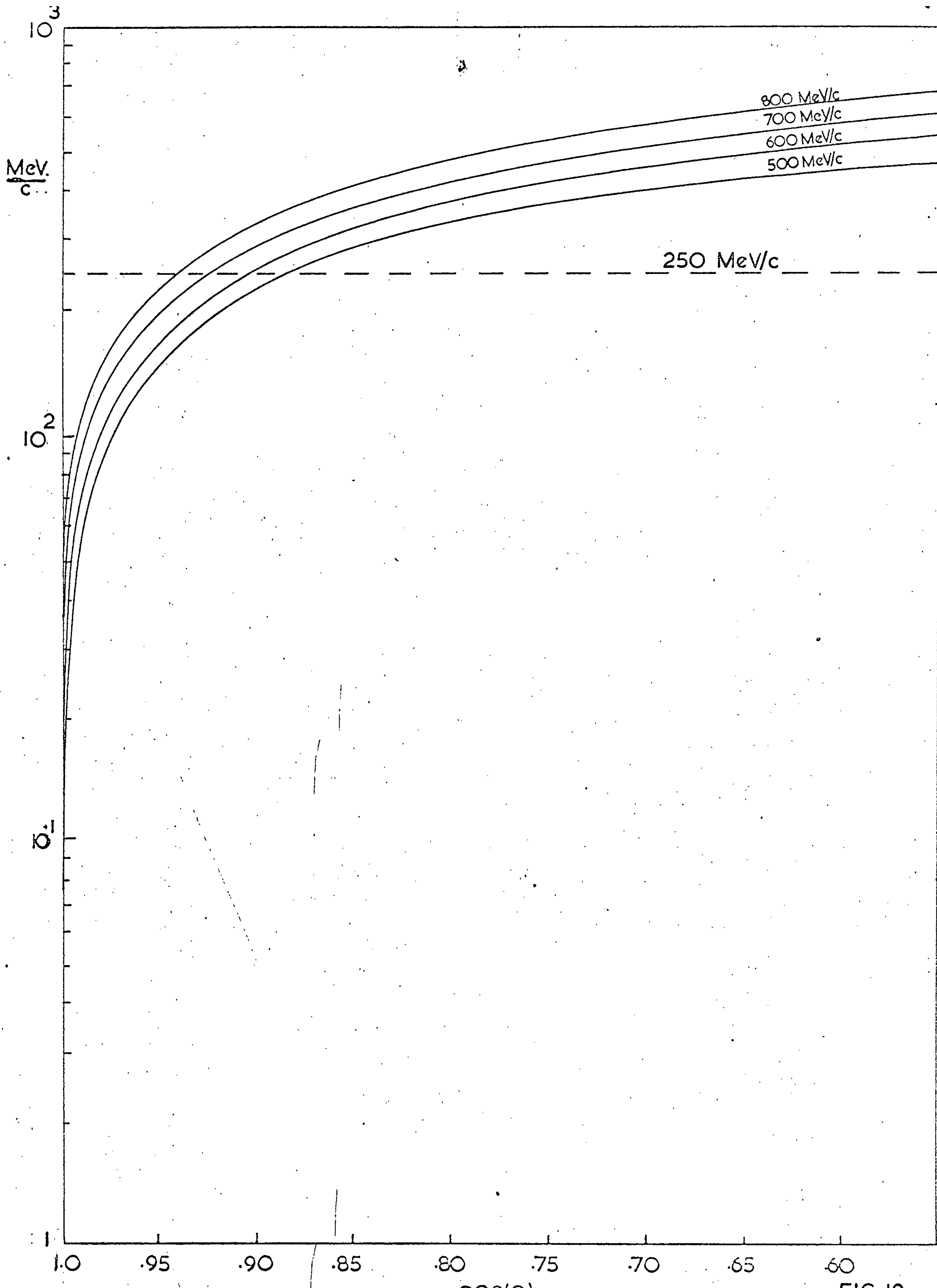

10^3
MeV.
c
800 MeV/c
700 MeV/c
600 MeV/c
500 MeV/c
250 MeV/c
10^2
10^1
1
1.0
·95
·90
·85
·80
·75
·70
·65
·60
COS(Θ)

FIG. 19

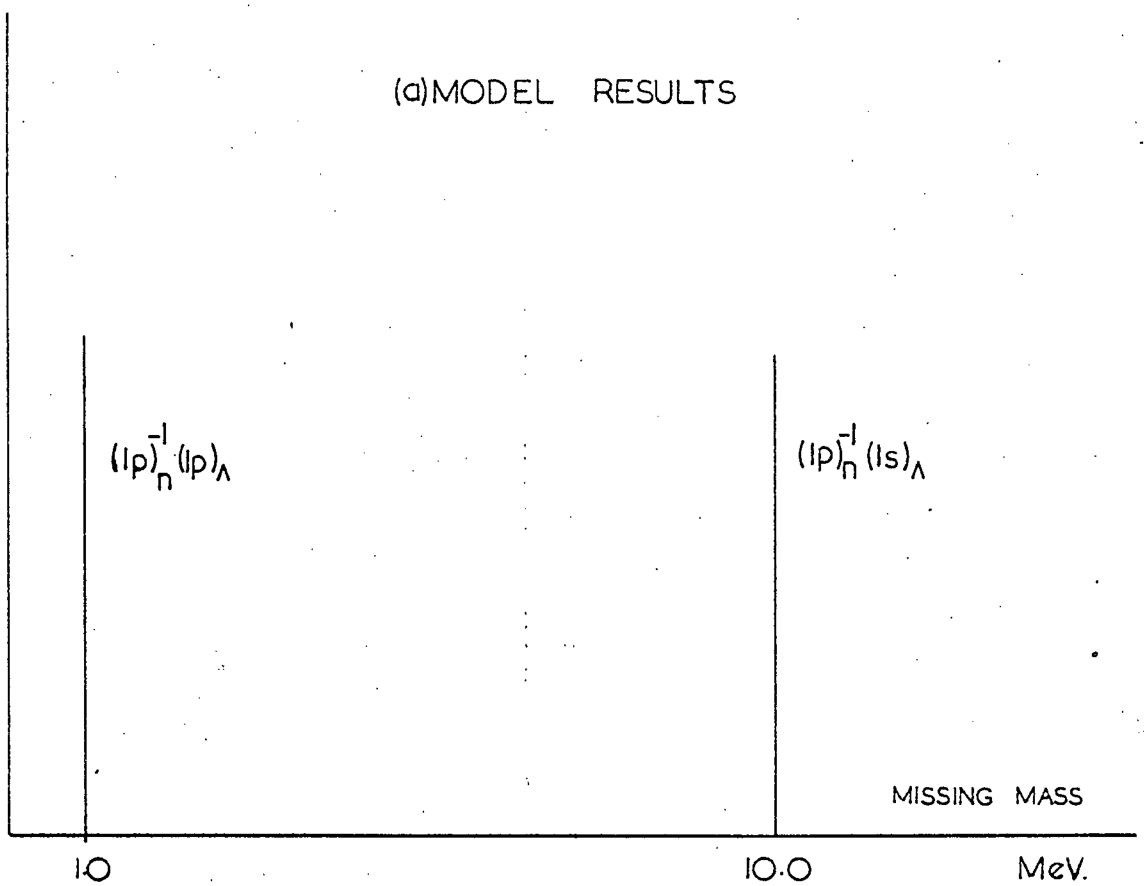
(a) MODEL RESULTS
$(1p)_n^{-1}(1p)_\Lambda$
$(1p)_n^{-1}(1s)_\Lambda$
MISSING MASS
1.0
10.0
MeV.

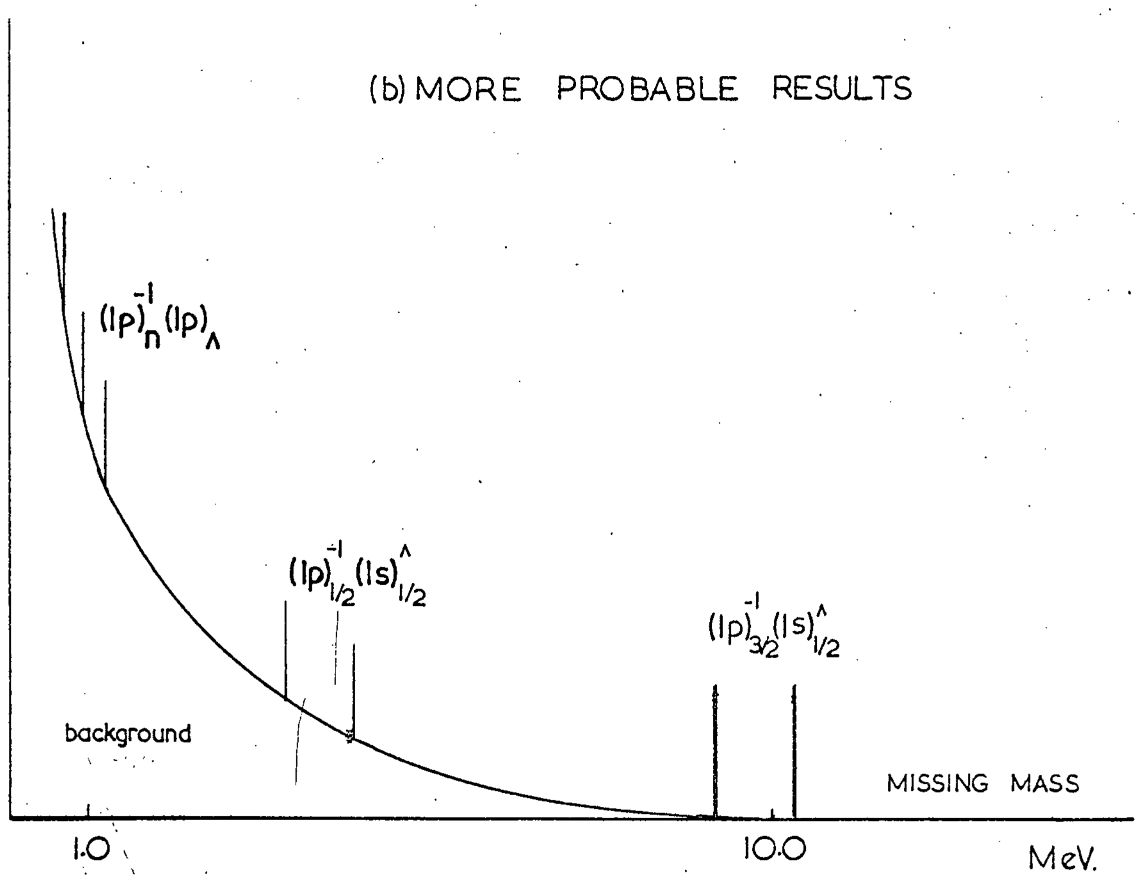
(b) MORE PROBABLE RESULTS
$(1p)_n^{-1}(1p)_\Lambda$
$(1p)_{1/2}^{-1}(1s)_{1/2}^{\Lambda}$
$(1p)_{3/2}^{-1}(1s)_{1/2}^{\Lambda}$
background
MISSING MASS
1.0
10.0
MeV.

FIG. 20